Systems/Circuits

5-HT_{2C} Receptor Knockdown in the Amygdala Inhibits Neuropathic-Pain-Related Plasticity and Behaviors

Guangchen Ji,[1] Wei Zhang,[1] Lenin Mahimainathan,[1] Madhusudhanan Narasimhan,[1] Takaki Kiritoshi,[1] Xiuzhen Fan,[3] Jigong Wang,[3] Thomas A. Green,[3] and Volker Neugebauer[1,2]

[1]Department of Pharmacology and Neuroscience and [2]Center of Excellence for Translational Neuroscience and Therapeutics, Texas Tech University Health Sciences Center, Lubbock, Texas 79430, and [3]Department of Pharmacology and Toxicology, The University of Texas Medical Branch, Galveston, Texas 77555

Neuroplasticity in the amygdala drives pain-related behaviors. The central nucleus (CeA) serves major amygdala output functions and can generate emotional-affective behaviors and modulate nocifensive responses. The CeA receives excitatory and inhibitory inputs from the basolateral nucleus (BLA) and serotonin receptor subtype 5-HT_{2C}R in the BLA, but not CeA, has been implicated anxiogenic behaviors and anxiety disorders. Here, we tested the hypothesis that 5-HT_{2C}R in the BLA plays a critical role in CeA plasticity and neuropathic pain behaviors in the rat spinal nerve ligation (SNL) model. Local 5-HT_{2C}R knockdown in the BLA with stereotaxic injection of 5-HT_{2C}R shRNA AAV vector decreased vocalizations and anxiety- and depression-like behaviors and increased sensory thresholds of SNL rats, but had no effect in sham controls. Extracellular single-unit recordings of CeA neurons in anesthetized rats showed that 5-HT_{2C}R knockdown blocked the increase in neuronal activity (increased responsiveness, irregular spike firing, and increased burst activity) in SNL rats. At the synaptic level, 5-HT_{2C}R knockdown blocked the increase in excitatory transmission from BLA to CeA recorded in brain slices from SNL rats using whole-cell patch-clamp conditions. Inhibitory transmission was decreased by 5-HT_{2C}R knockdown in control and SNL conditions to a similar degree. The findings can be explained by immunohistochemical data showing increased expression of 5-HT_{2C}R in non-GABAergic BLA cells in SNL rats. The results suggest that increased 5-HT_{2C}R in the BLA contributes to neuropathic-pain-related amygdala plasticity by driving synaptic excitation of CeA neurons. As a rescue strategy, 5-HT_{2C}R knockdown in the BLA inhibits neuropathic-pain-related behaviors.

Key words: amygdala; depression; pain; plasticity; serotonin

Significance Statement

Neuroplasticity in the amygdala has emerged as an important pain mechanism. This study identifies a novel target and rescue strategy to control abnormally enhanced amygdala activity in an animal model of neuropathic pain. Specifically, an integrative approach of gene transfer, systems and brain slice electrophysiology, behavior, and immunohistochemistry was used to advance the novel concept that serotonin receptor subtype 5-HT_{2C} contributes critically to the imbalance between excitatory and inhibitory drive of amygdala output neurons. Local viral vector-mediated 5-HT_{2C}R knockdown in the amygdala normalizes the imbalance, decreases neuronal activity, and inhibits neuropathic-pain-related behaviors. The study provides valuable insight into serotonin receptor (dys)function in a limbic brain area.

Introduction

The serotonergic system plays an important role in pain modulation (Heinricher et al., 2009; Ossipov et al., 2010) and selective serotonin reuptake inhibitors (SSRIs) can relieve neuropathic pain, but efficacy is weak and inconsistent (Dworkin et al., 2010; Lee and Chen, 2010; Finnerup et al., 2015). Serotonin can have inhibitory or excitatory effects in descending pathways depending on the receptor subtype (Ossipov et al., 2010). The family of at least 14 serotonin (5-HT) receptor subtypes is divided into seven groups based on their structural and functional characteristics

Received Aug. 3, 2016; revised Nov. 28, 2016; accepted Dec. 20, 2016.

Author contributions: G.J., T.A.G., and V.N. designed research; G.J., W.Z., L.M., M.N., X.F., J.W., and T.A.G. performed research; G.J., W.Z., T.K., X.F., T.A.G., and V.N. analyzed data; G.J., T.A.G., and V.N. wrote the paper.

This work was supported by National Institute of Neurological Disorders and Stroke–National Institutes of Health (Grants NS081121 and NS038261).

The authors declare no competing financial interests.

Correspondence should be addressed to Volker Neugebauer, M.D., Ph.D., Professor and Chair, Department of Pharmacology and Neuroscience, Director, Center of Excellence for Translational Neuroscience and Therapeutics, Texas Tech University Health Sciences Center (TTUHSC), School of Medicine, 3601 4th Street, Lubbock, TX 79430-6592. E-mail: volker.neugebauer@ttuhsc.edu.

DOI:10.1523/JNEUROSCI.2468-16.2016

 0270-6474/17/371378-16$15.00/0

(Bockaert et al., 2006; Hannon and Hoyer, 2008; Millan et al., 2008). The 5-HT$_{2C}$ receptor (5-HT$_{2C}$R) has emerged as a therapeutic target for neuropsychiatric disorders (Heisler et al., 2007; Christianson et al., 2010; Jensen et al., 2010), but 5-HT$_{2C}$R has also been implicated in adverse effects of 5-HT and SSRIs (Jensen et al., 2010) and in inconsistent clinical efficacy of SSRIs in neuropathic pain (Brasch-Andersen et al., 2011). 5-HT$_{2C}$R is expressed in GABAergic, glutamatergic, and dopaminergic neurons (Liu et al., 2007; Bubar et al., 2011). 5-HT$_{2C}$R mRNA and protein are found in many brain areas, including the amygdala and particularly its basolateral nucleus (Pompeiano et al., 1994; Clemett et al., 2000).

The amygdala plays a key role in fear and anxiety (Phelps and LeDoux, 2005) and in emotional-affective aspects of pain (Neugebauer, 2015). The amygdala circuitry that contributes to pain and pain modulation is centered on the lateral–basolateral (LA-BLA) and central (CeA) nuclei (Neugebauer et al., 2004; Neugebauer, 2015). The CeA serves major amygdala output functions and receives nociceptive information through the spino-parabrachio-amygdaloid pathway and highly processed affect-related information from the LA-BLA network (Neugebauer, 2015). Amygdala neuroplasticity in inflammatory pain is characterized by increased excitatory drive (Neugebauer et al., 2003; Han and Neugebauer, 2004; Bird et al., 2005; Han et al., 2005b; Fu and Neugebauer, 2008; Adedoyin et al., 2010; Cheng et al., 2011) and loss of inhibitory control of the CeA (Ren and Neugebauer, 2010; Ren et al., 2013). Neuroplasticity in the amygdala has also been found in neuropathic pain models (Ikeda et al., 2007; Gonçalves et al., 2008; Gonçalves and Dickenson, 2012; Nakao et al., 2012), but underlying mechanisms remain to be determined.

The present study tested the novel hypothesis that 5-HT$_{2C}$R in the BLA contributes to neuropathic-pain-related plasticity in the amygdala output region (CeA) and that knockdown of 5-HT$_{2C}$R can block pain-related behaviors. In support of our hypothesis, the BLA receives a strong serotonergic projection from the dorsal raphe nucleus (Ma et al., 1991; Lowry, 2002; Fernandez et al., 2016) and there is evidence for increased 5-HT release in the BLA, but not CeA, in aversive states (Funada and Hara, 2001; Macedo et al., 2005; Christianson et al., 2010). 5-HT$_{2C}$R in the BLA, but not CeA, contributes critically to anxiogenic behavior (Campbell and Merchant, 2003; Heisler et al., 2007; Christianson et al., 2010) and mediates anxiogenic side effects of acutely administered antidepressants such as SSRIs (Burghardt et al., 2007; Lee and Chen, 2010; Ravinder et al., 2011). We reported recently that a 5-HT2CR antagonist in the BLA, but not CeA, enabled a systemic SSRI to inhibit pain behaviors in an arthritis model (Grégoire and Neugebauer, 2013).

Synaptic and cellular effects of 5-HT$_{2C}$R in the amygdala are largely unknown. Acute 5-HT or a 5-HT$_2$ agonist activated GABAergic interneurons in the BLA, but higher concentrations or prolonged application seemed to have disinhibitory effects on BLA output (Rainnie, 1999). 5-HT$_{2C}$R activation facilitated NMDA-receptor-mediated synaptic plasticity in BLA pyramidal neurons (Chen et al., 2003). Here, we used a viral-vector-based strategy (adeno-associated viral mediated RNA interference, shRNA) for local (BLA) knockdown of 5-HT$_{2C}$R and evaluated the electrophysiological and behavioral effects in the rat model of neuropathic pain.

Materials and Methods

Animals

Male Sprague Dawley rats (120–320 g for brain slice physiology and 250–350 g for behavior and systems electrophysiology, corresponding to ~5–12 weeks of age; Harlan Laboratories) were housed in a temperature-controlled room under a 12 h light/dark cycle. Water and food were available without restriction. On the day of the experiment, rats were transferred from the animal facility and allowed to acclimate to the laboratory for at least 1 h. All experimental procedures were approved by the Institutional Animal Care and Use Committees at Texas Tech University Health Sciences Center and the University of Texas Medical Branch and conform to the guidelines of the International Association for the Study of Pain and of the National Institutes of Health. Experiments were performed in a blinded fashion so that the experimenter performing behavioral assays or electrophysiology *in vivo* or brain slice physiology was not aware of the pain condition (see "Neuropathic pain model") and intervention (see "Viral vector for 5-HT$_{2C}$R knockdown").

Neuropathic pain model

The well established spinal nerve ligation model (Bennett et al., 2003) was used, which provides stable and long-lasting neuropathic pain behaviors. Rats were anesthetized with isoflurane (3–4% induction, 2% maintenance). Under anesthesia and using sterile techniques, the L5 spinal nerve was tightly ligated using 6-0 sterile silk. In the sham operated group, the nerve was exposed but not ligated.

Viral vector for 5-HT$_{2C}$R knockdown

For local (basolateral amygdala, BLA) knockdown of 5-HT$_{2C}$R, recombinant AAV (type 2) vectors expressing a short hairpin RNA (shRNA) directed at the 5-HT$_{2C}$R or a control hairpin were used (Anastasio et al., 2014; Anastasio et al., 2015). The shRNA expression is driven by a mouse U6 promoter (pol III) so as not to compete with the pol II-driven expression cassette using a cytomegalovirus (CMV) promoter to express eGFP as a reporter. AAV vectors were packaged using a helper-free AAV packaging system (Agilent) with human embryonic kidney cells (HEK293). Vector was purified using an iodixanol gradient and ultra-centrifugation. The product of the gradient underwent a buffer exchange procedure to remove the iodixanol and further concentrate/purify the virus. The final virus in PBS had a titer of $\sim 10^{12}$ viral particles/ml. 5-HT$_{2C}$R or control shRNA-eGFP AAV2 vector (1 μl) was injected stereotaxically into the BLA of rats anesthetized with isoflurane (3–4% induction, 2% maintenance) in oxygen, two weeks after neuropathic or sham surgery. The following coordinates were used: 2.5 mm caudal to bregma, 4.8 mm lateral, 8.0–8.5 mm depth. In some animals, 5-HT$_{2C}$R shRNA-eGFP AAV2 vector (1 μl) was injected stereotaxically into the CeA as a control and to test our hypothesis that the site of action of 5-HT$_{2C}$R is in the BLA rather than CeA. The following coordinates were used for the CeA: 2.5 caudal to bregma, 4.0 lateral, 7.5–8.0 depth. Rats recovered for 2 weeks before the behavioral and electrophysiological studies to allow stable transgene expression. The knockdown and control vectors coexpress enhanced green fluorescent protein (eGFP) for easy identification of transduced cells.

Validation of 5-HT$_{2C}$R knockdown

qPCR. Brains were extracted and the BLA dissected out for mRNA analysis. The RNA was extracted by homogenizing in RNA STAT-60 (Teltest, Friendswood, TX), separating RNA from DNA and protein using chloroform, and precipitating the total RNA with isopropanol. Contaminating DNA was removed (TURBO DNA-Free, Life Technologies, CA) and 5 μg of the purified RNA was reverse transcribed into cDNA (Invitrogen SuperScript III First Strand Reverse Transcription kit). The resultant cDNA was quantified via qPCR using a SYBR Green method (Zhang et al., 2014).

Immunohistochemistry. Animals were deeply anesthetized with sodium pentobarbital (100 mg/kg, i.p.). Paraformaldehyde, 4% (w/v) in PBS was used for transcardial perfusion. Coronal slices (40 μm) containing the amygdala (−1.6 to −3.3 mm from bregma) were obtained with a cryostat at −20oC (Leica CM 1850, Leica Microsystems Nussloch GmbH, Nussloch, Germany). The sections were free-floating for blocking, antibody exposure and washes. PBS with 0.1% Triton X-100 plus 5% normal donkey serum was used for blocking of nonspecific binding for 1 h at 22°C. Sections were incubated with anti-5-HT$_{2C}$R antibody (goat, 1:200 dilution, Abcam, ab32887) in PBS+5% normal donkey serum overnight at 4°C and then washed with 0.1% Triton X-100 in PBS 5 × 10

min. Then sections were incubated with Alexa Fluor 555 donkey anti-goat IgG (Life Technologies, A-21432), 1:2500 dilution into PBS+5% normal donkey serum+0.1% Triton X-100 for 90 min at 22°C, washed with 0.1% Triton X-100 in PBS 5 × 10 min, and mounted onto microscope slides. Slides were stored in the dark at room temperature to air dry overnight (Anastasio et al., 2014). Slides were dehydrated and DPX mounting medium (EMS, Hatfield, PA) was used to complete the mounting process. The images were captured using SPE confocal with a Leica DMI4000 microscope (Leica Microsystems, Mannheim, Germany), and were analyzed with LAS AF software (Version 3.2.0).

Western blot analysis. Right BLA tissues were homogenized in radioimmunoprecipitation assay buffer containing protease inhibitor mixture (Sigma-Aldrich) using Omni tissue disrupter at 4°C and incubated on ice for 30 min. After centrifugation at 15,000 × *g* for 20 min, the supernatant was used for immunoblot assay. In brief, 40 μg of equal amounts of lysates from various treated groups were resolved by electrophoresis on 4–12% Bis-Tris gel (Invitrogen), electrotransferred to a polyvinylidene difluoride membrane, and blocked with 10% nonfat dry milk for 2 h. After overnight incubation with primary antibodies against 5-HT_{2c}R (1/1000; ab133570, Abcam) and GAPDH (1/1000; sc25778, Santa Cruz Biotechnologies, Santa Cruz, CA), the membranes were then washed three times in PBS-Tween 20 and incubated with horseradish peroxidase-conjugated anti-rabbit IgG (1:5000, Cell Signaling Technology, Beverly, MA) for 1 h. The antigen-antibody complex was detected using an ECL chemiluminescence kit (Pierce, Rockford, IL). 5-HT_{2C}R peptide (2 μg of peptide-ab170038/ml 1:1000 5-HT_{2c}R primary antibody; Abcam) was used to validate the specificity of the antibody. 5-HT_{2C}R protein signal (predicted molecular weight 52 kDa, apparent molecular weight of ~62 kDa) was analyzed by scanning densitometry using ImageJ software (NIH) and normalized to GAPDH.

5-HT_{2C}R expression changes in pain model

Immunostaining was conducted to detect 5-HT_{2C}R and GABA expression in BLA cells. Rats were deeply anesthetized with sodium pentobarbital (60 mg/kg, i.p.) and transcardially perfused with 200 ml of PBS (PBS; 8 g of NaCl, 1.44 g of Na_2HPO_4, 240 mg of KH_2PO_4, 200 mg of KCl in 1 L of dH_2O, pH 7.40) and then with 300 ml of a 4% paraformaldehyde PBS solution. Whole brains were collected and postfixed in 4% paraformaldehyde overnight at 4°C and then cryoprotected in a 30% sucrose PBS solution until they sank (~36–48 h). 40 μm coronal sections containing the BLA were collected using a cryostat set to −23°C. Free-floating sections were washed 3× in PBS and then incubated in 0.3% Triton X-100 and 10% goat serum (S26–100ml, EMD Millipore Corporation) for 30 min. Slices were incubated with the following primary antibodies at 37°C for 30 min and then at 4°C for 72 h: mouse anti-5-HT_{2C}R (D-12, sc-17797, 1:200, Santa Cruz Biotechnology Inc, Dallas, TX) and rabbit anti-GAD65+GAD67 antibody (ab11070, 1:500, abcam). Slices were then washed three times in PBS and incubated with the following secondary antibodies for 60 min at 37°C protected from light: goat anti-mouse IgG (1:100, TRITC, AP503R, EMD Millipore Corporation) and goat anti-rabbit IgG (1:200, FITC, ab6717, abcam). Slices were then washed three times in PBS for 10 min each and mounted onto slides with Vectashield Fluorescent Mounting Medium (Vector Laboratories). Brain tissue expression of the two fluorescence tagged antibodies (anti-5-HT_{2C}R, red; anti-GAD, green) and colocalization (yellow) were visualized and photographed using a Nikon Confocal Microscope with digital imaging software. Labeled cells were counted using ImageJ software (NIH). Primary antibodies were omitted for controls to verify signal and determine noise.

Behavior

Two weeks after neuropathic or sham surgery, 5-HT_{2C}R or control shRNA-eGFP AAV2 vector (1 μl) was infused into the BLA (see "Viral vector"). Rats recovered for 2 weeks to allow for stable transgene expression. The following behavioral assays were performed in shielded temperature- and light-controlled rooms.

Spinal reflexes were measured as mechanical withdrawal thresholds, using von Frey monofilaments (3.61, 3.84, 4.08, 4.31, 4.56, 4.74, 4.93, and 5.18, corresponding to 0.4, 0.6, 1, 2, 4, 6, 8, and 15 g) applied to the plantar surface of the hindpaw at the base of the third or fourth toe, the most sensitive area in spinal nerve ligation (SNL). An abrupt withdrawal of the foot during stimulation or immediately after stimulus removal was counted as a positive response. Thresholds were determined by the up-down method and the formula of Dixon (Dixon, 1980; Chaplan et al., 1994).

Vocalizations in the audible and ultrasonic (25 ± 4 kHz) ranges were measured using a condenser microphone and a bat detector, respectively, which were placed in front of the animal at a fixed distance (Han et al., 2005a; Neugebauer et al., 2007). Animals were anesthetized briefly with isoflurane (2%) and placed in a custom-designed recording chamber with openings for head and limbs. After habituation to the chamber, mechanical stimuli of innocuous (100 g/6 mm^2) and noxious (500 g/6 mm^2) intensities were applied to the hindpaw (15 s) using a calibrated forceps with a force transducer to monitor the applied force (in g). Durations of audible and ultrasonic vocalizations were analyzed for 1 min using Ultravox 2.0 software (Noldus Information Technology).

The elevated plus maze (EPM) test was used to measure anxiety-like behavior as described previously (Ji et al., 2007; Neugebauer et al., 2007). The EPM (Columbus Instruments) has two enclosed and two open arms arranged in a plus shape. The animal was placed onto the central area of the plus maze facing an open arm. Animal movements in the open and closed arms was detected by photocells and recorded for 15 min using a computerized analysis system (Multi-Varimex software; Columbus Instruments). Anxiety-like behavior was analyzed as the ratio of open-arm entries to the total number of entries (expressed as a percentage) during the first 5 min, as is standard EPM protocol (Walf and Frye, 2007).

Sucrose preference was measured to model anhedonia (Fernando and Robbins, 2011). Animals were preexposed to a sucrose solution (1% w/v) for 3 d (1 h/d). Two days later, sucrose versus water consumption (in milliliters) from two bottles in the home cage was measured for 15 min. Sucrose preference was expressed as percentage of total consumption. Preference for a familiar sucrose solution is a measure of natural reward as opposed to neophobia.

Systems electrophysiology

Two weeks after neuropathic or sham surgery, 5-HT_{2C}R or control shRNA-eGFP AAV2 vector (1 μl) was infused into the BLA (see "Viral vector"). Rats recovered for 2 weeks to allow for stable transgene expression. Extracellular single-unit recordings were made from neurons in the laterocapsular division of the CeA (CeLC) as described previously (Ji and Neugebauer, 2009; Ji et al., 2010; Ji et al., 2015).

Animal preparation and anesthesia. Rats were anesthetized with pentobarbital (induction, 50 mg/kg, i.p.; maintenance, 15 mg/kg/h, i.v.), paralyzed with vecuronium (induction, 0.3- 0.5 mg, iv; maintenance, 0.3 mg/h, iv), and artificially ventilated (3–3.5 ml; 55–65 strokes/min). End-tidal CO_2 levels (kept at 4.0 ± 0.2%) and heart rate (using ECG) were monitored continuously. Core body temperature was maintained at 37°C by means of a homeothermic blanket system. The animal was mounted in a stereotaxic frame (Kopf Instruments) and a craniotomy was performed at the sutura frontoparietalis level to allow the insertion of the recording electrode.

Single-unit recording and identification of CeA neurons. Individual neurons were recorded with glass insulated carbon filament electrodes (4–6 MΩ) using the following coordinates: 2.2–3.1 mm caudal to bregma, 3.8–4.2 mm lateral to midline, depth 7–8.5 mm. The recorded signals were amplified, band-pass filtered (300 Hz to 3 kHz), displayed on an analog oscilloscope, and processed by an interface (1401 Plus; CED). Spike2 software (version 4; CED) was used for spike sorting, data storage, and analysis of single-unit activity. Spike size and configuration were monitored continuously. Only those neurons with a spike configuration that matched a preset template and could be clearly discriminated from activity in the background throughout the experiment were included in the study. Neurons in the lateral CeA were identified by monitoring background activity and responses to mechanical compression of the tissue at innocuous (100 g/6 mm^2) and noxious (500 g/6 mm^2) intensities with a calibrated forceps (see "Vocalizations"). Noxious compression was used sparingly as a search stimulus. Once a neuron was found that responded to noxious stimuli, the size and thresholds of the receptive

fields in deep tissue and skin were mapped using graded mechanical stimuli of innocuous and noxious intensities. Neurons were selected that had a receptive field in the hindpaw (innervation territory of L5) and responded more strongly to noxious than innocuous mechanical stimuli. One neuron was recorded per animal to avoid biasing the sample and to allow for verification of the recording site using electrolytic lesion (see "Verification of recording site").

Firing pattern analysis. Spike2 software was used to measure neuronal activity as spikes/second for 10 min (background activity in the absence of intentional stimulation) or 15 s (mechanical compression). For the analysis of net evoked activity, background activity was measured for 1–3 min before the stimulation sequence of innocuous and noxious mechanical compression of the tissue. The mean value (spikes/second) was then subtracted from the total activity during stimulation to obtain net evoked activity. Spike2 software burst analysis script was used to analyze interspike interval (ISI) distribution and burst-like activity for each CeA neuron. Burst-like activity was defined as follows: before the first spike in a burst, there was a preceding silent period of at least 100 ms, which was then followed by a second spike with an ISI of ≤10 ms (Weyand et al., 2001; Wang et al., 2006). Any subsequent spikes with preceding ISI ≤10 ms were also considered to be part of a burst. The variation in the ISIs is described by using the coefficient of variation (CV2) (Holt et al., 1996). CV2 was computed by assessing the SD and mean firing for two adjacent ISIs [CV2 = 2(ISI2 − ISI1)/(ISI2 + ISI1)]. The CV2 for each pair of adjacent ISIs was plotted against the mean of those two ISIs. Small CV2 values indicate regular firing, whereas large CV2 values (≥1) indicate irregular firing. The average CV2 values were calculated for each experimental group (SNL/sham with 5-HT$_{2C}$R/control shRNA vector).

Verification of recording site. At the end of each experiment, the recording site in the CeA was marked by injecting DC (250 μA for 3 min) through the carbon filament recording electrode. The brain was removed and submerged in 10% formalin and potassium ferrocyanide. Tissues were stored in 30% sucrose before they were frozen sectioned at 50 μm. Sections were stained with hematoxylin and eosin (H&E), mounted on gel-coated slides, and coverslipped. The boundaries of the different amygdala nuclei were easily identified under the microscope. Lesion/recording sites were verified histologically and plotted on standard diagrams.

Brain slice electrophysiology

Brain slice preparation. Coronal (400 μm) brain slices containing the CeA and LA-BLA were obtained from neuropathic or sham rats 2 weeks after stereotaxic injection of 5-HT$_{2C}$R or control shRNA-eGFP AAV2 vector (1 μl) into the BLA (see "Viral vector"). As described previously (Ji et al., 2013; Ren et al., 2013; Ji et al., 2015), brains were quickly removed and immersed in oxygenated ice-cold sucrose-based physiological solution containing the following (in mM): 87 NaCl, 75 sucrose, 25 glucose, 5 KCl, 21 $MgCl_2$, 0.5 $CaCl_2$, and 1.25 NaH_2PO_4. Brain slices were prepared using a Vibratome (Series 1000 Plus; The Vibratome Company). Brain slices were then incubated in oxygenated artificial CSF (ACSF) at room temperature (21°C) for at least 1 h before patch recordings. ACSF, pH 7.4, contained the following (in mM): 117 NaCl, 4.7 KCl, 1.2 NaH_2PO_4, 2.5 $CaCl_2$, 1.2 $MgCl_2$, 25 $NaHCO_3$, and 11 glucose. A single brain slice was transferred to the recording chamber and submerged in ACSF (31 ± 1°C) superfusing the slice at ~2 ml/min. Only one or two brain slices per animal were used. Only one neuron was recorded in each slice. Numbers in the text refer to the number of neurons tested for each parameter.

Patch-clamp recording. Whole-cell voltage-clamp recordings were made from visually identified neurons in the CeLC using DIC-IR videomicroscopy as described previously (Ren et al., 2013; Ji et al., 2015). Patch electrodes had tip resistances of 3–6 MΩ. The following internal solution was used (in mM): 122 K-gluconate, 5 NaCl, 0.3 $CaCl_2$, 2 $MgCl_2$, 1 EGTA, 10 HEPES, 5 Na_2-ATP, and 0.4 Na_3-GTP, pH adjusted to 7.2–7.3 with KOH and osmolarity to 280 mOsm/kg with sucrose. Data acquisition and analysis was done using a dual 4-pole Bessel filter (Warner Instruments), low-noise Digidata 1322 interface (Axon Instruments, Molecular Devices), Axoclamp-2B amplifier (Axon Instruments), and pClamp9 software (Axon Instruments). Head-stage voltage was monitored continuously on an oscilloscope to ensure precise performance of the amplifier. If series resistance (monitored with pClamp9 software) changed >10%, the neuron was discarded.

Synaptic transmission. EPSCs and IPSCs were evoked in CeLC neurons by focal electrical stimulation (150 μs square-wave pulses; using an S88 stimulator; Grass Technologies) in the BLA using a concentric bipolar stimulation electrode (Kopf Instruments). EPSCs and IPSCs were recorded at −70 and 0 mV, respectively. The calculated equilibrium potential for chloride in this system was −68.99 mV (Nernst equation, pClamp9 software). Monosynaptic EPSCs were completely blocked by NBQX (10 μM). IPSCs were blocked by bicuculline (10 μM) or NBQX (10 μM), consistent with feedforward inhibition in the BLA–CeA pathway (Ren et al., 2013). Drugs were purchased from Tocris Bioscience (Techne Corporation). Input–output (I/O) relationships were obtained by measuring peak amplitudes of EPSCs and IPSCs as a function of stimulation intensity (100 μA steps).

Statistical analysis

All averaged values are given as the mean ± SE. Statistical significance was accepted at the level $p < 0.05$. GraphPad Prism 5.0 software was used for all statistical analyses. Statistical analysis was performed on the raw data. Student's *t* test was used to compare two sets of data that had Gaussian distribution and similar variances. For multiple comparisons, one-way or two-way ANOVA (repeated measures where appropriate) was used with Bonferroni correction and *post hoc* tests as indicated in the text and figure legends.

Results

The goal of this study was to test the hypothesis that knockdown of serotonin receptor 5-HT$_{2C}$R in the BLA would inhibit neuropathic-pain-related plasticity in the amygdala output region (CeA) and pain-related behaviors. The right amygdala was targeted because of evidence for right-hemispheric lateralization in several pain models (Carrasquillo and Gereau, 2007; Carrasquillo and Gereau, 2008; Ji and Neugebauer, 2009; Gonçalves and Dickenson, 2012).

Viral-vector-mediated knockdown of 5-HT$_{2C}$R expression in the BLA

We first validated the viral vector strategy by measuring 5-HT$_{2C}$R mRNA via PCR and 5-HT$_{2C}$R protein expression with immunohistochemistry and Western blotting (see Materials and Methods). Figure 1*A* shows vector transduction as eGFP fluorescence in BLA neurons of the right amygdala. AAV2 5-HT$_{2C}$R shRNA injected into the BLA *in vivo* decreased 5-HT$_{2C}$ receptor mRNA significantly ($p < 0.05$, unpaired *t* test) compared with AAV2 control shRNA (Fig. 1*B*). To investigate this efficacy cell by cell, immunohistochemistry was performed on tissue transduced with 5-HT$_{2C}$R or control shRNA vector. For the control vector (Fig. 1*C–E*), there was considerable colocalization of eGFP and 5-HT$_{2C}$R immunofluorescence (blue arrows), whereas the 5-HT$_{2C}$R shRNA vector (Fig. 1*F–H*) clearly decreased immunofluorescence for the receptor in transduced cells. Quantitative analysis of 5-HT$_{2C}$R protein expression using Western blotting (Fig. 1*I,J*) showed that 5-HT$_{2C}$R shRNA vector decreased 5-HT$_{2C}$R expression in the BLA of sham ($n = 3$) and SNL ($n = 2$) rats significantly compared with sham ($n = 3$) and SNL ($n = 2$) rats treated with control vector ($F_{(3,8)} = 68.68$, ANOVA with Bonferroni *post hoc* tests). SNL increased 5-HT$_{2C}$R protein expression in rats treated with control shRNA, but not in rats treated with 5-HT$_{2C}$R shRNA vector ($n = 2$). Tissues were obtained 2 weeks after stereotaxic injections of 5-HT$_{2C}$R knockdown vector or control shRNA vector; that is, 4 weeks after SNL/sham surgery.

5-HT$_{2C}$R knockdown in the BLA inhibits neuropathic-pain-related behaviors

We next tested the ability of AAV2 knockdown of 5-HT$_{2C}$R in the BLA to block behavioral changes in an animal model of neuropathic pain (SNL; see Materials and Methods). Nocifensive reflexes (Fig. 2*A*,*B*), vocalizations (Fig. 2*C*), anxiety-like (Fig. 3*A*), and depression-like (Fig. 3*B*) behaviors were measured in SNL and sham control rats. Nocifensive reflexes were measured repeatedly before and after sham/SNL surgery and before and after stereotaxic injections of 5-HT$_{2C}$R or control shRNA vector into the amygdala. Vocalizations and anxiety- and depression-like behaviors were measured only one time in each animal (2 weeks after stereotaxic injections of 5-HT$_{2C}$R knockdown vector or control shRNA vector; that is, 4 weeks after SNL/sham surgery). Locations of the injection sites into BLA and CeA (control) are shown in Figure 4.

Nocifensive reflexes

Hindlimb withdrawal thresholds were measured with von Frey filaments of different force (see Materials and Methods) before and 3, 7, 14, 21, 28, and 35 d after SNL or sham surgery. Figure 2*A* shows that mechanical thresholds in sham rats did not change after sham surgery, but remained at a threshold of 15 g, which is the cutoff point for mechanical threshold determination with this method. In sham rats, 5-HT$_{2C}$R knockdown ($n = 12$ rats) or control vector ($n = 13$ rats) in the BLA had no significant effect ($F_{(6,66)} = 0.6431$ and $F_{(6,72)} = 1.897$, respectively; $p > 0.05$, repeated-measures ANOVA). In contrast, SNL rats showed decreased mechanical thresholds from day 3 on ($F_{(6,84)} = 25.69$; $p < 0.001$, repeated-measures ANOVA). In SNL rats, stereotaxic injections of AAV 5-HT$_{2C}$R shRNA ($n = 17$ rats), but not control vector ($n = 15$ rats), into the BLA increased the withdrawal thresholds 2 and 3 weeks after AAV injection significantly ($F_{(3,53)} = 54.35$, $p < 0.001$, Bonferroni correction, knockdown vector compared with control vector). 5-HT$_{2C}$R shRNA vector injection into the CeA (Fig. 2*B*) did not change mechanosensitivity in sham controls ($n = 5$) and did not block mechanical hypersensitivity of SNL rats ($n = 5$). The decreased mechanical thresholds of SNL were significantly different from those of sham controls ($F_{(1,48)} = 1427.00$, $p < 0.001$, two-way repeated-measures ANOVA with Bonferroni *post hoc* tests). The data show that SNL surgery produces stable, long-lasting mechanical hypersensitivity and that 5-HT$_{2C}$R knockdown in the BLA, but not CeA, has significant antinociceptive effects.

Vocalizations

Audible and ultrasonic vocalizations (Fig. 2*C*) were evoked by brief (15 s) noxious mechanical stimulation of the affected hindpaw as described in Materials and Methods. Total duration of vocalizations was measured for 1 min in the following experimental groups (also subjected to von Frey tests). Sham controls with stereotaxic injection of 5-HT$_{2C}$R knockdown vector ($n = 12$ rats) or control vector ($n = 12$ rats) into the BLA; in SNL rats with stereotaxic injection of 5-HT$_{2C}$R knockdown vector ($n = 12$ rats) or control vector ($n = 12$ rats) into the BLA; and SNL rats with stereotaxic injection of 5-HT$_{2C}$R knockdown vector into the CeA ($n = 5$ rats). Measurements were made 2 weeks after vector injection; that is, 4 weeks after SNL/sham surgery. 5-HT$_{2C}$R knockdown had no significant effect in sham rats ($p > 0.05$, ANOVA with Bonferroni correction compared with control vector). SNL rats showed higher vocalizations than sham controls ($p < 0.001$, comparing rats with control vector injection). 5-HT$_{2C}$R knockdown in the BLA of SNL rats inhibited audible and ultrasonic vocalizations significantly (audible $F_{(4,48)} = 11.01$, ultrasonic $F_{(4,48)} = 10.32$, $p < 0.05$ and $p < 0.01$, ANOVA with Bonferroni

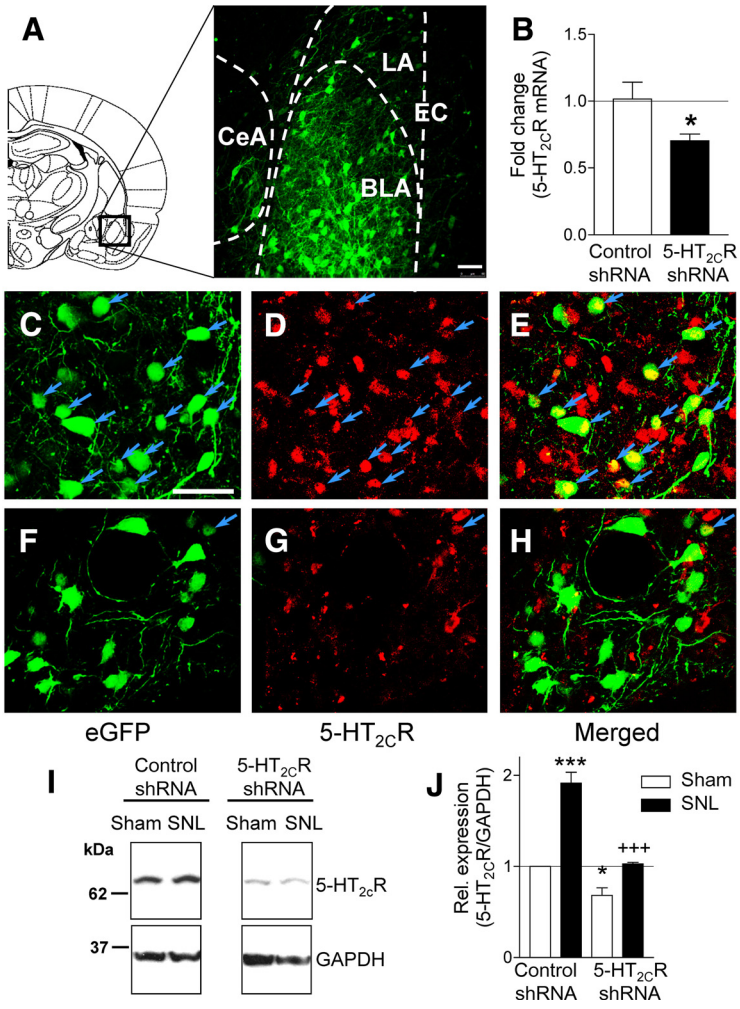

Figure 1. AAV2-mediated knockdown of 5-HT$_{2C}$R expression in the BLA. ***A***, Diagram of a coronal brain slice (2.30 mm caudal to bregma) indicates the amygdala area shown in the confocal image (20× objective) of vector transduction (eGFP fluorescence) in the BLA. White bar represents 50 μm. EC, External capsule. ***B***, *In vivo* knockdown of 5-HT$_{2C}$R mRNA measured via qPCR. *$p < 0.05$, unpaired *t* test. ***C–E***, Confocal images (40× objective) show expression of control vector eGFP (***C***; green) and 5-HT$_{2C}$R (***D***; red) and colocalization (***E***; merged view). Blue arrows denote neurons with colocalized eGFP and 5-HT$_{2C}$R. White bar in ***C*** represents 50 μm. ***F–H***, 40× images showing expression of 5-HT$_{2C}$R-shRNA knockdown vector eGFP (***F***; green) and 5-HT$_{2C}$R (***G***; red), and lack of colocalization (***H***; merged view), validating viral-vector-mediated 5-HT$_{2C}$R knockdown. Data in ***A–H*** are from sham rats. ***I***, ***J***, Quantitative analysis of 5-HT$_{2C}$R protein expression. Representative cropped images of Western blot analysis using 5-HT$_{2C}$R antibody on right BLA tissue lysates treated as indicated. GAPDH antibody was used to normalize the 5-HT$_{2C}$R signal. Bar graph (means ± SE) shows quantification of the 5-HT$_{2C}$R/GAPDH protein. 5-HT$_{2C}$R shRNA vector reduced 5-HT$_{2C}$R protein expression in SNL and sham controls. Sham, $n = 3$ rats; SNL, $n = 2$ rats. *,***$p < 0.05$, 0.001 compared with control shRNA in shams; $^{+++}p < 0.001$ compared with control shRNA in SNL, ANOVA with Bonferroni *post hoc* tests.

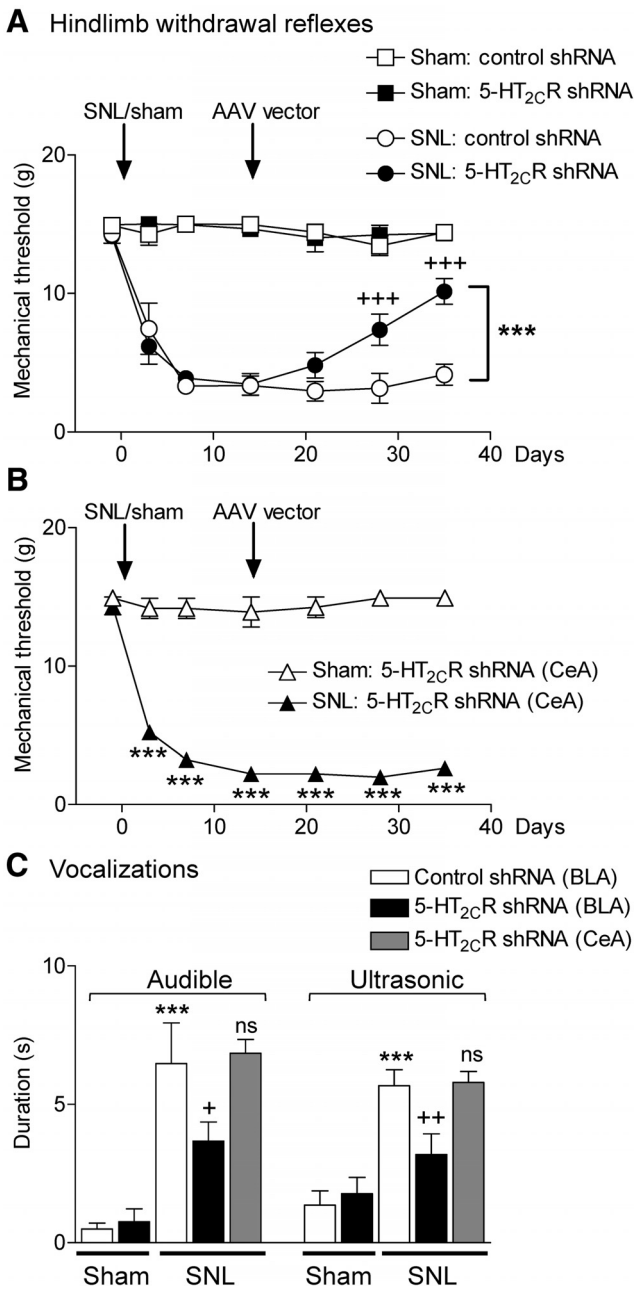

Figure 2. 5-HT$_{2C}$R knockdown in the BLA inhibits nocifensive reflexes (***A***, ***B***) and vocalizations (***C***) of neuropathic rats. ***A***, ***B***, Mechanical thresholds (left paw) were measured with von Frey filaments repeatedly before and after sham/SNL surgery and before and after 5-HT$_{2C}$R/control shRNA AAV2 vector injection into the BLA (***A***) or CeA (***B***). ***A***, Sham rats with control vector ($n = 13$ rats) or 5-HT$_{2C}$R knockdown vector ($n = 12$ rats) injected into the BLA showed no changes. In SNL rats, 5-HT$_{2C}$R shRNA ($n = 17$ rats), but not control vector ($n = 15$ rats), in the BLA increased the withdrawal thresholds significantly. Symbols show means ± SEM $^{+++}p < 0.001$ compared with presurgery; $^{***}p < 0.001$ compared with control vector; two-way repeated-measures ANOVA with Bonferroni correction. ***B***, 5-HT$_{2C}$R shRNA vector injected into the CeA of sham or SNL rats had no effect on the significant changes of mechanical thresholds after SNL surgery ($n = 5$) compared with sham controls ($n = 5$). $^{***}p < 0.001$, SNL compared with sham; two-way repeated-measures ANOVA with Bonferroni correction. ***C***, Audible and ultrasonic vocalizations evoked by brief (15 s) noxious mechanical compression (500 g/6 mm^2) of the left paw with a calibrated forceps. In sham rats, there was no difference between 5-HT$_{2C}$R knockdown ($n = 12$ rats) or control ($n = 12$ rats) vector into the BLA. In SNL rats, 5-HT$_{2C}$R knockdown vector in the BLA ($n = 12$ rats) inhibited vocalizations compared with control vector ($n = 12$ rats). 5-HT$_{2C}$R knockdown vector into the CeA ($n = 5$ rats) had no effect. Measurements were made 2 weeks after vector injection; that is, 4 weeks after SNL/sham surgery. $^{***}p < 0.001$ compared with sham; $^{+,++}p < 0.05$, 0.01 compared with control vector; ns, nonsignificant, ANOVA with Bonferroni correction.

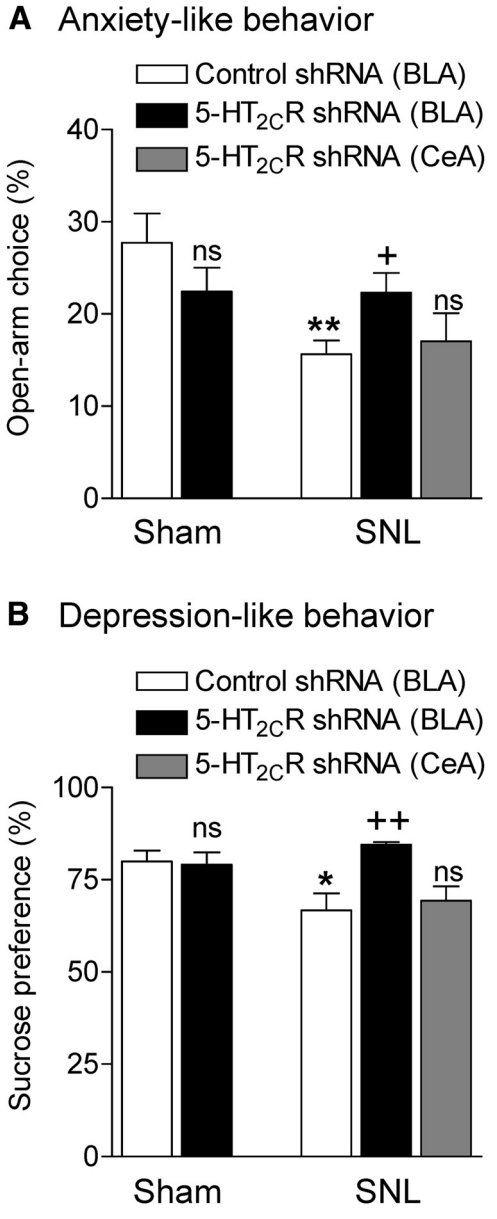

Figure 3. 5-HT$_{2C}$R knockdown in the BLA inhibits anxiety-like (***A***) and depression-like (***B***) behaviors of neuropathic rats. ***A***, Open-arm preference on the EPM was measured during the first 5 min. In sham controls, injection of 5-HT$_{2C}$R shRNA vector into the BLA ($n = 11$ rats) had no significant effect compared with control vector ($n = 15$ rats). In SNL rats, 5-HT$_{2C}$R knockdown in the BLA ($n = 16$ rats) increased open-arm choice compared with control vector ($n = 17$ rats). 5-HT$_{2C}$R shRNA vector injected into the CeA ($n = 5$ rats) had no significant effect. ***B***, Sucrose preference in sham controls was not different between rats injected with 5-HT$_{2C}$R knockdown vector ($n = 6$ rats) and control vector ($n = 10$ rats) into the BLA. SNL rats showed decreased sucrose preference ($n = 9$ rats, injected with control vector). 5-HT$_{2C}$R knockdown in the BLA increased sucrose preference ($n = 5$ rats). Injection of 5-HT$_{2C}$R shRNA vector into the CeA ($n = 5$ rats) had no effect. ***A***, ***B***, Measurements made 2 weeks after vector injection; that is, 4 weeks after SNL/sham surgery. $^{*,**}p < 0.05$, 0.01, SNL compared with sham; $^{+,++}p < 0.05$, 0.01, 5-HT$_{2C}$R shRNA compared with control shRNA vector; ns, nonsignificant, ANOVA with Bonferroni correction.

correction). Importantly, 5-HT$_{2C}$R knockdown in the CeA had no significant effect. The data suggest that the viral vector knockdown strategy is specific to 5-HT$_{2C}$R in the BLA.

Anxiety-like behavior

Open-arm preference (entries) on the EPM was measured during the first 5 min as described in Materials and Methods in the

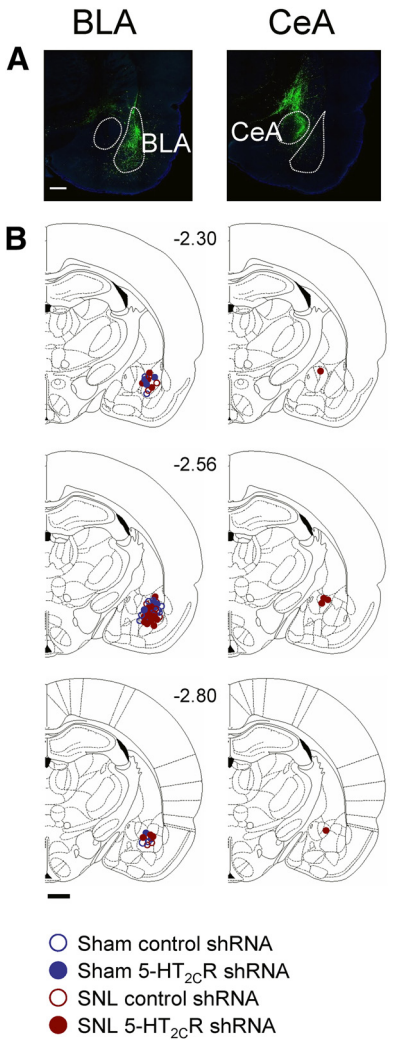

Figure 4. Location of viral vector injection sites. ***A***, Confocal images of eGFP fluorescence of vector injected into the BLA (left) and CeA area (offsite control, right). Scale bar, 500 μm. ***B***, Diagrams showing coronal brain slices. Numbers indicate distance from the bregma. Symbols show the positions of the needle tips for AAV2 vector injections into BLA (left) and CeA (right). Scale bar, 500 μm.

following experimental groups (Fig. 3*A*): sham controls with stereotaxic injection of 5-HT$_{2C}$R knockdown vector ($n = 11$ rats) or control vector ($n = 15$ rats) into the BLA, SNL rats with stereotaxic injection of 5-HT$_{2C}$R knockdown vector ($n = 16$ rats) or control vector ($n = 17$ rats) into the BLA, and SNL rats with stereotaxic injection of 5-HT$_{2C}$R knockdown vector into the CeA ($n = 5$ rats). Measurements were made 2 weeks after vector injection; that is, 4 weeks after SNL/sham surgery. Note that all animals were tested for mechanical hypersensitivity but some are not included in Figure 2*A* because a complete time course study was not done. 5-HT$_{2C}$R knockdown had no significant effect in sham rats ($p > 0.05$, ANOVA with Bonferroni correction compared with control vector). SNL rats showed decreased open-arm preference, indicating anxiogenic effects of the pain model and 5-HT$_{2C}$R knockdown in the BLA, but not CeA, of SNL rats increased open-arm preference significantly ($F_{(4,59)} = 3.967$, ANOVA; $p < 0.01$, Bonferroni *post hoc* test comparing SNL and sham rats injected with control vector; $p < 0.05$, comparing SNL rats with and without 5-HT$_{2C}$R knockdown). The data suggest that 5-HT$_{2C}$R knockdown in the BLA has anxiolytic effects in the neuropathic pain model.

Depression-related behavior

Sucrose preference (Fig. 3*B*) was measured as described in Materials and Methods in the following experimental groups that were also tested for mechanical hypersensitivity (Fig. 2*A*,*B*): sham controls with stereotaxic injection of 5-HT$_{2C}$R knockdown vector ($n = 6$ rats) or control vector ($n = 10$ rats) into the BLA, SNL rats with stereotaxic injection of 5-HT$_{2C}$R knockdown vector ($n = 5$ rats) or control vector ($n = 9$ rats) into the BLA, and SNL rats with stereotaxic injection of 5-HT$_{2C}$R knockdown vector into the CeA ($n = 5$ rats). Measurements were made 2 weeks after vector injection; that is, 4 weeks after SNL/sham surgery. Sham animals showed preference for sucrose and 5-HT$_{2C}$R shRNA vector had no significant effect ($p > 0.05$, ANOVA with Bonferroni correction compared with control vector). SNL rats showed decreased sucrose preference, which is consistent with depression-like effects of the pain model and 5-HT$_{2C}$R knockdown in the BLA, but not CeA, of SNL rats increased sucrose preference significantly ($F_{(4,30)} = 4.008$, ANOVA; $p < 0.05$, Bonferroni *post hoc* test comparing SNL and sham rats with control vector; $p < 0.01$, comparing SNL rats with and without 5-HT$_{2C}$R knockdown). The data suggest that 5-HT$_{2C}$R knockdown in the BLA has antidepressant-like effects in the neuropathic pain model.

5-HT$_{2C}$R knockdown in the BLA inhibits neuronal activity of CeA neurons in a neuropathic pain model

Our previous work showed that responsiveness and activity of neurons in the amygdala output region (CeA) drives pain-related behaviors and CeA neurons receive excitatory and inhibitory inputs from the BLA (Neugebauer, 2015). Therefore, we sought to determine whether 5-HT$_{2C}$R knockdown in the BLA can inhibit activity of CeA neurons in the SNL model of neuropathic pain. Extracellular single unit recordings of CeA neurons were made in SNL and sham rats 2 weeks after stereotaxic injections of 5-HT$_{2C}$R or control shRNA vector; that is, 4 weeks after SNL/sham surgery (Figs. 5, 6). Recording sites in the laterocapsular division of the CeA are shown in Figure 7. CeA neurons were selected that responded more strongly to noxious than innocuous stimuli. Background activity and responses to innocuous and noxious compression of the hindpaw with a calibrated forceps (see Materials and Methods) increased significantly in SNL rats ($n = 11$ neurons) compared with sham controls ($n = 10$ neurons; background activity, $F_{(3,47)} = 5.346$; innocuous stimulation, $F_{(3,47)} = 8.763$; noxious stimulation, $F_{(3,47)} = 6.989$; $p < 0.01$–0.001, ANOVA with Bonferroni correction comparing control vector-treated SNL and sham rats). Individual examples are shown in Figure 5, *A* and *C*. Data are summarized in Figure 5*E*. Knockdown of 5-HT$_{2C}$R in the BLA of SNL rats inhibited background and evoked activity of CeA neurons ($n = 13$) significantly ($p < 0.05$–0.001, ANOVA with Bonferroni correction) compared with CeA neurons ($n = 17$) recorded in SNL rats treated with control vector (Fig. 5*C*,*D*, individual examples; Fig. 5*E*, summary).

Our previous work (also see Neugebauer et al., 2004; Ji and Neugebauer, 2009) showed that the receptive field size of CeA neurons increased in a model of arthritis pain, indicating changes in the central processing of afferent input. Therefore, we determined the effects of neuropathic pain and 5-HT$_{2c}$R knockdown on the receptive field of CeA neurons by mapping size of the receptive fields using graded mechanical stimuli of innocuous and noxious intensities. For quantification of receptive field size, the body map was divided into 25 different sectors (Fig. 5*G*) as described before (Ji and Neugebauer, 2009). The total number of areas that contained part of the receptive field of a neuron was

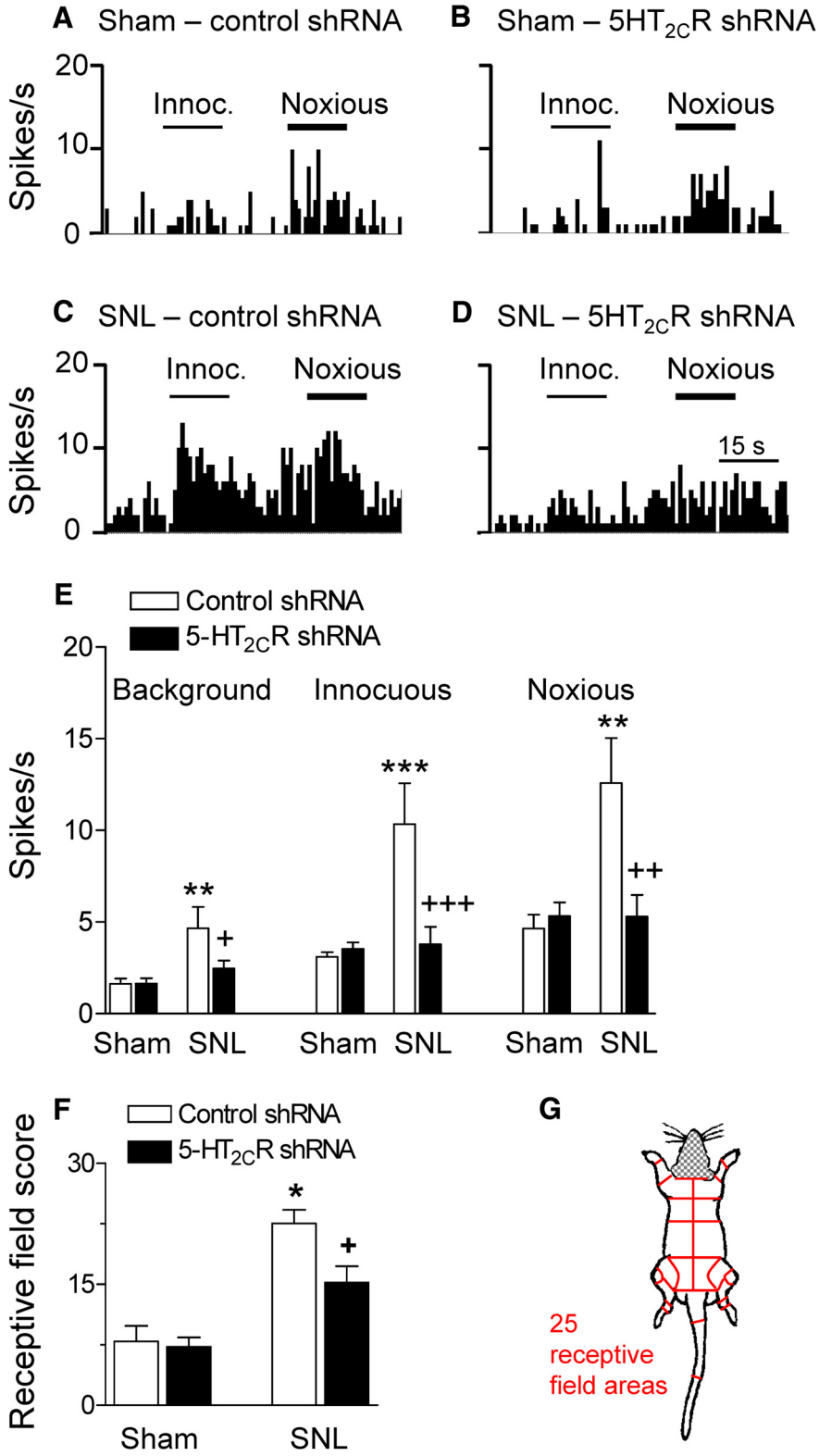

Figure 5. 5-HT$_{2C}$R knockdown in the BLA inhibits activity of CeA neurons in neuropathic rats. ***A–D***, Examples of individual CeA neurons (four different neurons). Peristimulus time histograms (PSTHs) show the number of action potentials (spikes) per second. Innocuous (100 g/6 mm^2) and noxious (500 g/6 mm^2) stimuli (compression of the hindpaw) are indicated by horizontal lines. ***A***, CeA neuron recorded in a sham rat injected with control vector into BLA. ***B***, CeA neuron in a sham rat with 5-HT$_{2C}$R knockdown in BLA. ***C***, CeA neuron in an SNL rat with control vector injected into BLA. ***D***, CeA neuron in an SNL rat with 5-HT$_{2C}$R knockdown in BLA. ***E***, Summary. Bar histograms show mean ± SE for the sample of neurons. Background activity and net evoked responses to innocuous and noxious stimuli increased significantly in (control-vector-treated) SNL rats ($n = 11$ neurons) compared with (control vector treated) shams ($n = 10$ neurons). $^{**,***}p < 0.01, 0.001$, ANOVA with Bonferroni correction. 5-HT$_{2C}$R shRNA vector injected into BLA ($n = 13$ neurons) decreased background and evoked activity significantly compared with control vector ($n = 17$ neurons). $^{+,++,+++}p < 0.05–0.001$, ANOVA with Bonferroni correction. ***F***, ***G***, Receptive field size calculated for each neuron as the number of body areas (total of 25, see map in ***G***) from which the neuron could be activated (Ji and Neugebauer, 2009). Head and neck areas were not tested because of the recording situation. Bar histograms show receptive field scores for the sample of neurons (same number of neurons as in ***E***). Receptive field size of CeA neurons in SNL rats was significantly larger than that of neurons in sham rats; $^{*}p < 0.05$, ANOVA with Bonferroni correction. 5-HT$_{2C}$R shRNA vector in the BLA decreased receptive field size of CeA neurons in SNL rats significantly compared with neurons in SNL rats with control vector. $^{+}p < 0.05$, ANOVA with Bonferroni correction.

calculated and averaged for neurons in sham and SNL rats treated with 5-HT$_{2C}$R knockdown and control vector (Fig. 5*F*). Head and neck were not assessed because of the recording situation. Receptive fields were symmetrical and included the hindpaws. The average receptive field size of CeA neurons in SNL rats ($n = 11$ neurons) was significantly larger than that of CeA neurons in sham rats ($n = 10$ neurons) and 5-HT$_{2C}$R knockdown in the BLA had no significant effect in sham rats ($n = 17$ neurons), but decreased the receptive field size of CeA neurons in SNL rats ($n = 13$ neurons) significantly ($F_{(3,48)} = 16.98$, ANOVA; $p < 0.05$, Bonferroni *post hoc* tests comparing neurons in SNL rats and in sham rats, treated with control vector; $p < 0.05$, comparing neurons in SNL rats with and without 5-HT$_{2C}$R knockdown). The data suggest that 5-HT$_{2C}$R in the BLA regulates responsiveness and inputs to CeA neurons in the neuropathic pain model.

For a more refined analysis of background activity changes in the neuropathic pain model and with 5-HT$_{2C}$R knockdown, we analyzed firing patterns (regular, irregular, bursting) in 48 CeA neurons belonging to four experimental groups: sham rats injected with 5-HT$_{2C}$R shRNA ($n = 17$ neurons) or control shRNA vector ($n = 11$) into the BLA and SNL rats injected with 5-HT$_{2C}$R shRNA ($n = 11$) or control shRNA vector ($n = 9$) into the BLA. Background activity is defined as action potential firing in the absence of any intentional stimulation. Figure 6 shows the analysis of CV2 and ISIs as described in Materials and Methods using Spike2 software. CV2 was calculated from the SD and mean firing for two adjacent ISIs to describe the variation in ISIs (Holt et al., 1996). Scatter plot analysis of CV2 for each pair of adjacent ISIs against the mean of those two ISIs showed that irregular firing (CV2 ≥ 1) of CeA

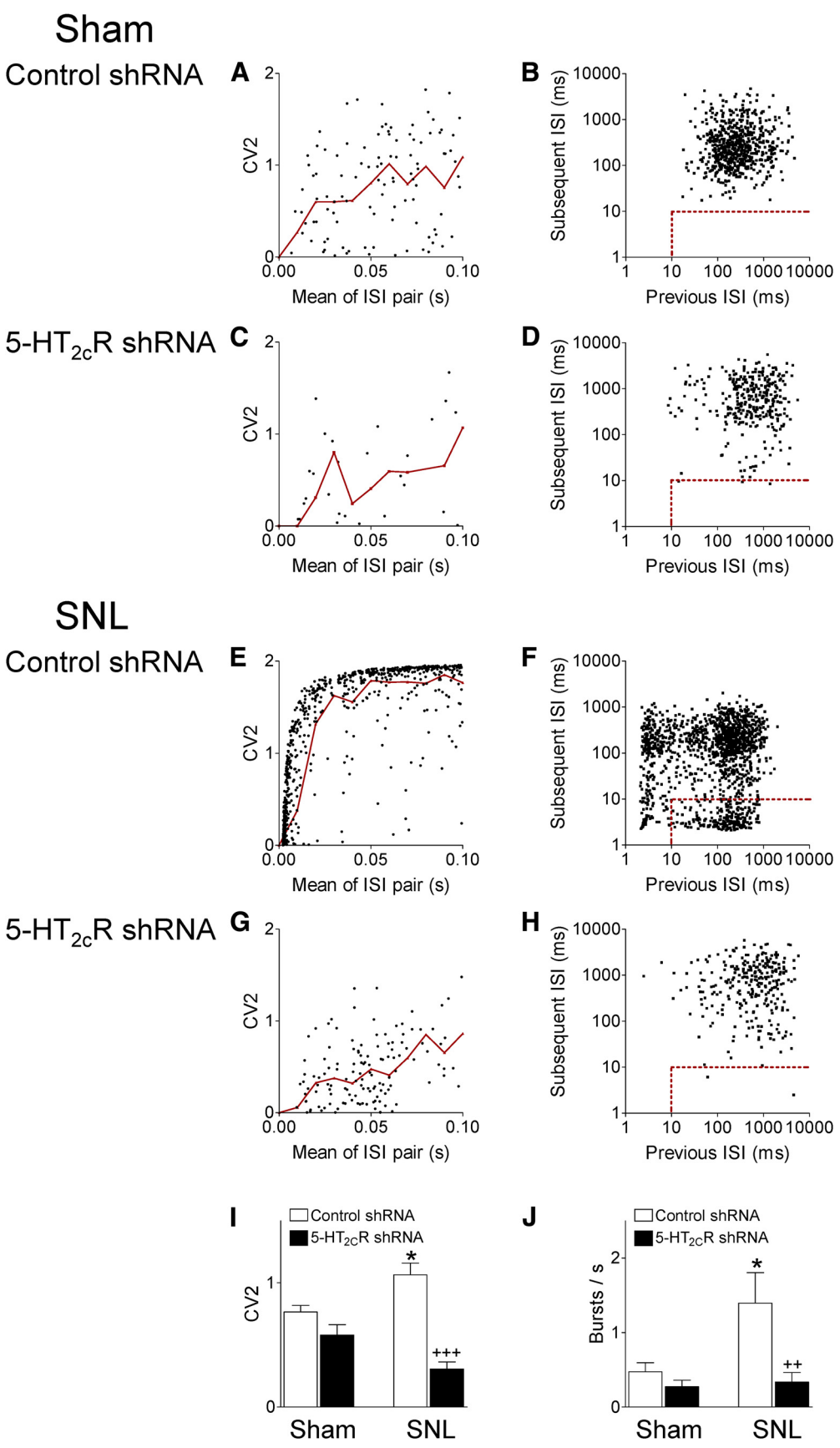

Figure 6. 5-HT$_{2C}$R knockdown in the BLA changes firing pattern of CeA neurons in neuropathic rats. CV2 of ISIs (left) and burst activity (right) were analyzed. ***A***, ***C***, ***E***, ***G***, Scatter plot analysis of CV2 for each pair of adjacent ISIs against the mean of those two ISIs shows regular (CV2 < 1) and irregular (CV2 ≥ 1) firing. Individual CeA neurons from different experimental groups (one neuron recorded in each per animal). Red lines show mean CV2 values in logarithmically spaced bins. ***I***, Bar histograms showing means $\pm$ SE of CV2 for each experimental group. Irregular firing of CeA neurons was significantly increased in neuropathic rats (SNL, $n = 9$ neurons) compared with shams ($n = 11$ neurons, $^*p < 0.05$, ANOVA with Bonferroni (*Figure legend continues.*)

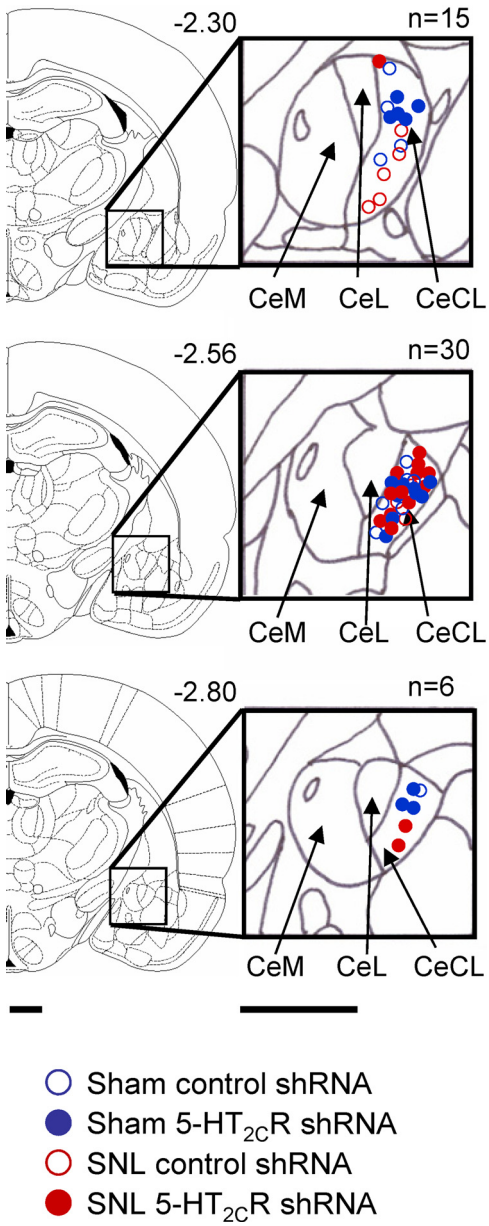

Figure 7. Location of recording sites. Diagrams show coronal brain slices. Numbers indicate distance from the bregma. Symbols show the positions of the tips of recording electrodes in the CeLC based on electrolytic lesions (see Materials and Methods). Scale bars, 500 μm.

neurons was increased in neuropathic rats (SNL) compared with shams. 5-HT$_{2C}$R knockdown in the BLA reduced the higher CV2 of CeA neurons in SNL rats significantly, but had no effect in sham rats (Fig. 6*A*, *C*, *E*, *G*, individual examples; Fig. 6*I*, summary of CV2 averaged for each experimental group; $F_{(3,44)} = 14.14$, ANOVA; $p < 0.05$, Bonferroni *post hoc* test comparing neurons in SNL and shams; $p < 0.001$, comparing neurons in SNL rats with and without 5-HT$_{2C}$R knockdown). Next, we analyzed bursting activity defined as follows. The first spike in a burst was preceded by a silent period of at least 100 ms and was followed by a second spike with an ISI ≤10 ms. Any subsequent spikes with preceding ISI ≤10 ms were also considered as part of a burst (see Materials and Methods). Joint ISI scatter plots (previous ISI against the subsequent ISI) showed significantly increased burst events (indicated by the rectangular insets in Fig. 6*B*, *D*, *F*, *H*) in CeA neurons recorded in SNL rats compared with sham controls. 5-HT$_{2C}$R knockdown in the BLA reduced the burst activity of CeA neurons in SNL rats significantly, but had no effect in sham rats (Fig. 6*B*, *D*, *F*, *H*, individual examples; Fig. 6*J*, summary of burst frequency averaged for each experimental group; $F_{(3,39)} = 7.118$, ANOVA; $p < 0.05$, Bonferroni *post hoc* test comparing neurons in SNL and sham rats; $p < 0.01$, comparing neurons in SNL rats with and without 5-HT$_{2C}$R knockdown). The data suggest that 5-HT$_{2C}$R drives irregular and burst firing of CeA neurons in the neuropathic pain model.

←

(*Figure legend continued.*) correction). 5-HT$_{2C}$R knockdown in the BLA decreased CV2 in CeA neurons in SNL rats ($n = 11$) significantly compared with control shRNA ($^{+++}p < 0.001$, ANOVA with Bonferroni correction), but had no effect in sham rats ($n = 17$). ***B***, ***D***, ***F***, ***H***, Joint ISI plots (previous ISI against the subsequent ISI) detected burst activity indicated by the rectangular insets (dots within the dashed red lines represent the first spike in a burst). Individual CeA neurons from different experimental groups (one neuron recorded in each per animal). ***J***, Bar histograms showing mean number of bursts for neurons in each experimental group (same number of neurons as in ***I***). Burst activity of CeA neurons was significantly higher in SNL rats compared with shams ($^{*}p < 0.05$, ANOVA with Bonferroni correction). 5-HT$_{2C}$R knockdown in the BLA decreased burst frequency in SNL rats significantly compared with control shRNA ($^{2+}p < 0.01$, ANOVA with Bonferroni correction), but had no effect in sham rats.

5-HT$_{2C}$R knockdown in the BLA inhibits enhanced synaptic excitation of CeA neurons in a neuropathic pain model

Neurons in the amygdala output region (CeA) receive direct excitatory input and feedforward inhibition from the BLA (Neugebauer, 2015). Using whole-cell patch-clamp recordings in brain slices, EPSCs and IPSCs were evoked in laterocapsular CeA neurons (Fig. 8) by focal electrical stimulation in the BLA, as in our previous studies (Ren et al., 2013). Monosynaptic EPSCs (recorded at −70 mV) were mediated by non-NMDA receptors because they were completely blocked by NBQX (10 μM). Polysynaptic IPSCs (recorded at 0 mV) were blocked by bicuculline (10 μM) or NBQX (10 μM), which is generally accepted as evidence for the concept of glutamate-driven feedforward inhibition (Ren et al., 2013). Brain slices were obtained from sham rats and SNL rats 2 weeks after stereotaxic injection of 5-HT$_{2C}$R or control shRNA vector into the BLA; that is, 4 weeks after SNL/sham surgery. I/O functions of synaptic transmission were determined by measuring peak amplitudes of EPSCs (Fig. 8*A*, *C*) and IPSCs (Fig. 8*B*, *D*) as a function of stimulation intensity (100 μA steps).

Excitatory transmission was significantly increased in slices from SNL rats ($n = 16$ neurons, Fig. 8*C*) compared with shams ($n = 16$, Fig. 8*A*; $p < 0.001$, $F_{(1,330)} = 48.66$, mean effect of intervention, two-way ANOVA, comparing data from control vector injected groups). 5-HT$_{2C}$R knockdown in the BLA decreased the enhanced excitatory transmission in CeA neurons from SNL rats ($n = 8$ neurons) compared with control vector ($n = 16$) significantly ($p < 0.001$, $F_{(1,242)} = 66.87$, main effect of treatment, two-way ANOVA; Fig. 8*C*). In CeA neurons from sham rats, 5-HT$_{2C}$R knockdown had a small but overall significant effect ($n = 16$ neurons; $p < 0.01$, $F_{(1,330)} = 9.07$, main effect of treatment, two-way ANOVA; Fig. 8*A*). However, *post hoc* analysis (Bonferroni correction) showed no significant difference between 5-HT$_{2C}$R and control shRNA vector treatment for any stimulus intensity.

Inhibitory transmission did not change significantly in slices from SNL rats ($n = 16$ neurons, Fig. 8*D*) compared with shams ($n = 13$, Fig. 8*B*; $p > 0.05$, $F_{(1,297)} = 1.60$, mean effect of intervention, two-way ANOVA, comparing data from control vector injected groups). 5-HT$_{2C}$R knockdown in the BLA decreased inhibitory transmission in CeA neurons from sham rats ($n = 16$

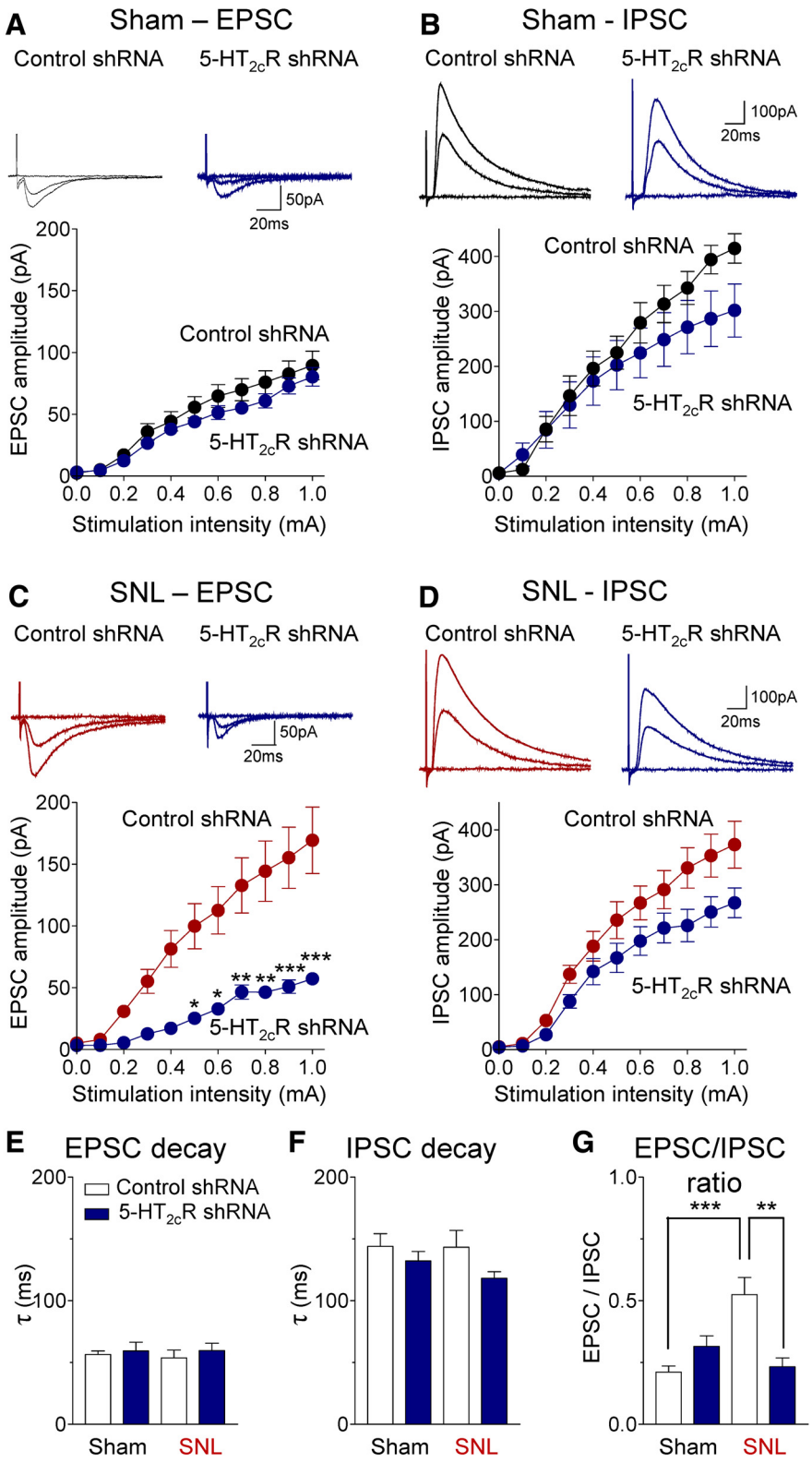

Figure 8. 5-HT$_{2C}$R knockdown in the BLA inhibits excitatory synaptic drive onto CeA neurons in brain slices from neuropathic rats. Excitatory and inhibitory postsynaptic currents (EPSCs, ***A***, ***C***; IPSCs, ***B***, ***D***) evoked by electrical stimulation in BLA were recorded in CeA neurons in brain slices from sham rats (***A***, ***B***) and SNL rats (***C***, ***D***). Brain slices were obtained 2 weeks after stereotaxic injection of 5-HT$_{2C}$R shRNA or control vector into the BLA; that is, 4 weeks after SNL or sham surgery. Traces show individual synaptic responses to stimulation with intensities of 0, 0.5 and 1.0 mA. Graphs show I/O functions obtained by plotting peak amplitude of EPSCs or IPSCs as a function of stimulus intensity (steps of 100 μA; see Materials and Methods and Results). ***A***, In CeA neurons from sham rats, 5-HT$_{2C}$R knockdown had little effect on excitatory transmission ($n = 16$ neurons) compared with control vector ($n = 16$ neurons). ***B***, 5-HT$_{2C}$R knockdown decreased inhibitory transmission ($n = 16$ neurons) compared with control vector ($n = 13$ neurons) in brain slices from sham rats. ***C***, In CeA neurons from SNL rats, 5-HT$_{2C}$R knockdown inhibited excitatory transmission significantly ($n = 16$ neurons) compared with control vector ($n = 8$ neurons). $^{*,**,***}p < 0.05–0.001$, two-way ANOVA with Bonferroni correction. ***D***, 5-HT$_{2C}$R knockdown decreased inhibitory transmission in CeA neurons from SNL rats ($n = 9$ neurons) compared with control vector ($n = 16$). See Results for details of the two-way ANOVA. ***E***, ***F***, No difference was found in decay time (tau) of EPSCs or IPSCs. ***G***, EPSC/IPSC ratio increased significantly in the SNL model ($n = 12$ neurons) compared with sham controls ($n = 12$) and was significantly decreased with 5-HT$_{2C}$R knockdown ($n = 7$ neurons) compared with control vector ($n = 16$) in the SNL model. ***E–G***, Data obtained with stimulation intensity of 1 0.0 mA. $^{**,***}p < 0.01, 0.001$, ANOVA with Bonferroni correction.

neurons, $p < 0.01$, $F_{(1,297)} = 6.62$, main effect of treatment, two-way ANOVA; Fig. 8*B*) and from SNL rats ($n = 9$ neurons, $p < 0.001$, $F_{(1,253)} = 21.69$, main effect of treatment, two-way ANOVA; Fig. 8*D*). However, *post hoc* analysis (Bonferroni correction) did not detect significant differences for individual stimulus intensities.

No effect on decay kinetics of EPSCs or IPSCs was found (Fig. 8*E*,*F*). Analysis of the EPSC/IPSC ratio (Fig. 8*G*) confirmed a significant shift toward excitatory drive of CeA neurons in the neuropathic pain model and a significant inhibitory effect of 5-HT$_{2C}$R knockdown in the BLA ($F_{(3,41)} = 7.853$, ANOVA), suggesting that this imbalance involves 5-HT$_{2C}$R in the BLA. In contrast to the 5-HT$_{2C}$R-mediated increase in excitatory transmission (Fig. 8*A*,*C*), contribution of 5-HT$_{2C}$R to synaptic inhibition (Fig. 8*B*,*D*) did not change in the pain model.

Increased 5-HT$_{2C}$R expression in non-GABAergic BLA cells in a neuropathic pain model

The results so far suggested that 5-HT$_{2C}$R in the BLA drives neuropathic pain behaviors by increasing activity in CeA neurons through a mechanism that involves a shift from synaptic inhibition to enhanced excitatory transmission. To determine the mechanism of this imbalance in neuropathic pain, we analyzed expression of 5-HT$_{2C}$R in GABAergic (GAD-positive) and non-GABAergic (Fig. 9) BLA cells. Immunohistochemistry using selective antibodies for 5-HT$_{2C}$R and GAD (see Materials and Methods) showed a significant increase ($p < 0.001$, unpaired t test) of 5-HT$_{2C}$R immunoreactivity in the BLA in coronal brain slices from SNL rats ($n = 6$ rats) compared with sham controls ($n = 6$ rats). The data are summarized in Figure 9*C*. Individual examples are shown in Figure 9*A*. Next, we analyzed colocalization of 5-HT$_{2C}$R in GAD-positive (pre-

sumed GABAergic) cells. 5-HT$_{2C}$R can be found on GABAergic and non-GABAergic cells (Carr et al., 2002; Liu et al., 2007), but this has not been shown for the BLA. In brain tissue from sham rats 5-HT$_{2C}$R was largely colocalized in GAD-positive cells and only 14% of BLA cells with 5-HT$_{2C}$R immunoreactivity were GAD negative (Fig. 9*B*). The percentage of non-GAD-positive cells expressing 5-HT$_{2C}$R increased significantly in BLA tissue from SNL rats (> 40% of BLA cells with 5-HT$_{2C}$R immunoreactivity; $p < 0.001$, unpaired t test, Fig. 9*D*). These data are consistent with an increase of 5-HT$_{2C}$R expression in neuropathic pain largely due to expression in non-GABAergic cells in the BLA such as pyramidal cells that are known to provide excitatory input to the CeA (Neugebauer, 2015).

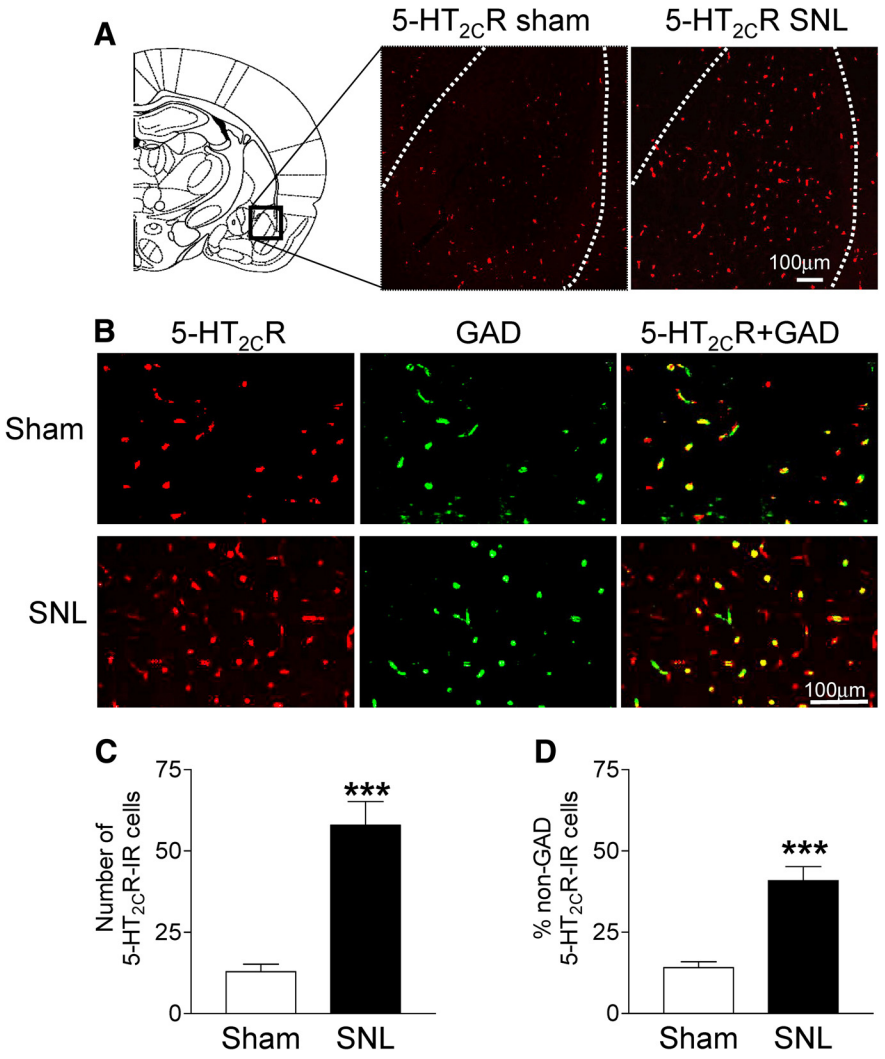

Figure 9. Changes of 5-HT$_{2C}$R expression in GAD-positive and GAD-negative BLA cells in the neuropathic pain model. ***A***, 5-HT$_{2C}$R antibody immunoreactivity (IR, red fluorescence) in the BLA in representative coronal sections from a sham rat and an SNL rat. ***B***, Confocal photomicrographs show 5-HT$_{2C}$R-IR (red), GAD-labeled GABAergic cells (green), and colocalization of 5-HT$_{2C}$R and GAD (yellow) in tissues from sham and SNL rats (top and bottom, respectively). ***C***, Number of 5-HT$_{2C}$R-IR BLA cells counted in tissues from six sham rats ($n = 18$ slices) and six SNL rats ($n = 18$ slices). ***D***, Percentage of non-GAD cells in the population of 5-HT$_{2C}$R-IR cells in the BLA of sham rats ($n = 9$ slices from $n = 6$ rats) and SNL rats ($n = 9$ slices from $n = 6$ rats). Coronal brain slices were 40 μm thick. See Materials and Methods for details. ***$p < 0.001$, unpaired t test.

Discussion

This study addressed the role of serotonin receptor 5-HT$_{2C}$R in the amygdala in a model of neuropathic pain. Serotonin plays an important role in pain modulation, but its pain-related actions in the amygdala remain to be determined. To fill this knowledge gap, an integrative approach of gene transfer (local viral-vector-mediated 5-HT$_{2C}$R knockdown), systems and brain slice electrophysiology, behavioral assays, and 5-HT$_{2C}$R immunohistochemistry was used. The results show that local 5-HT$_{2C}$R knockdown in the amygdala input region (BLA) inhibits neuronal activity in the amygdala output region (CeA) by normalizing the imbalance between excitatory drive and synaptic inhibition in a rat model of neuropathic pain (SNL). This imbalance resulted at least in part from increased 5-HT$_{2C}$R expression in non-GABAergic cells in the BLA. Therefore, 5-HT$_{2C}$R knockdown inhibited amygdala-driven neuropathic-pain-related behaviors.

5-HT$_{2C}$R and pain-related amygdala plasticity

The novel concept that serotonin receptor subtype 5-HT$_{2C}$R contributes critically to neuropathic-pain-related changes in amygdala activity and behaviors is important for a number of reasons. The amygdala has emerged as a key player in emotional-affective aspects of pain in acute and chronic models (for a recent review, see Neugebauer, 2015). Neuroplasticity in the amygdala output region correlates positively with pain behaviors, so controlling amygdala activity is a desirable therapeutic goal. The focus of this study on serotonin was based on the generally beneficial effects of serotonin in pain modulation (Heinricher et al., 2009; Ossipov et al., 2010) and the amygdala as a site of clinical effects of SSRIs in depressed patients (Godlewska et al., 2012; Bocchio et al., 2016). The results provide a mechanistic explanation for inconsistent or weak clinical efficacy of SSRIs in neuropathic pain (Dworkin et al., 2010; Lee and Chen, 2010; Finnerup et al., 2015) by showing that 5-HT$_{2C}$R contributes to enhanced amygdala activity and neuropathic pain behaviors. Adverse 5-HT$_{2C}$R function in the amygdala also serves as the neurobiological basis for our recent finding (Grégoire and Neugebauer, 2013) that a 5-HT$_{2C}$R antagonist (SB242084) in the amygdala (BLA) conveyed analgesic efficacy to a systemic SSRI (fluvoxamine). Likewise, SB242084 in the BLA blocked the anxiogenic effects of imipramine and fluoxetine (Vicente and Zangrossi, 2012). Greater pain relief with an SSRI in patients with peripheral neuropathic pain was associated with a single nucleotide polymorphisms in the 5-HT$_{2C}$R gene, possibly resulting in receptor malfunction (Brasch-Andersen et al., 2011).

Synaptic mechanisms

Our data suggest a change in expression pattern of 5-HT$_{2C}$R in the BLA. The BLA provides direct excitatory projections to CeA neurons (Duvarci and Pare, 2014). We found increased excitatory synaptic input, increased responsiveness, and irregular

and burst firing patterns in these neurons in a neuropathic pain model. Increased expression of 5-HT$_{2C}$R, a $G_{q/11}$ protein-coupled receptor (Hannon and Hoyer, 2008), in non-GABAergic BLA cells (Fig. 9) could explain the enhanced excitatory drive of CeA neurons from BLA in neuropathic pain. Glutamatergic pyramidal cells and distinct types of inhibitory GABAergic neurons are the two types of neurons found in the BLA (McDonald, 1998; Sah et al., 2003). Another possibility is that chronic or high release of serotonin disinhibits BLA output by reducing the excitatory drive onto BLA interneurons (Rainnie, 1999). Under normal conditions, 5-HT$_{2C}$R in the BLA is known to be expressed in GABAergic interneurons (see also Fig. 9) and mediates acute serotonin control of BLA projection neurons by activating interneurons (Bocchio et al., 2016), influencing precision and synchrony of BLA pyramidal cells (Ryan et al., 2012). Consistent with a change in BLA-5-HT$_{2C}$R-mediated synaptic drive onto CeA neurons in the pain model, the decay kinetics of excitatory and inhibitory synaptic responses did not change (Fig. 8). Changes in gating kinetics of (postsynaptic) receptors and/or spatiotemporal profile of transmitter concentration resulting, for example, from multivesicular release or changes in transmitter clearance would affect the decay times (Nusser et al., 2001). The amygdala receives strong serotonergic input from the midbrain dorsal raphe nucleus and 5-HT axons innervate pyramidal cells and interneurons densely in the BLA, but not CeA (Parent et al., 1981; Ma et al., 1991; Muller et al., 2007; Fernandez et al., 2016). 5-HT$_{2C}$R is localized postsynaptically to serotonergic axons (Pompeiano et al., 1994; Clemett et al., 2000). 5-HT levels were not measured in this study, so the (relative) contribution of changes in receptor expression and serotonin release to increased amygdala activity in neuropathic pain remains to be determined.

In contrast to the enhanced excitatory drive from BLA to CeA, GABAergic feedforward inhibition did not change in the neuropathic pain model. BLA projection cells providing direct excitatory or feedforward inhibitory input to CeA neurons belong to different subpopulations (Janak and Tye, 2015). To explain the 5-HT$_{2C}$R-mediated selective change in excitatory transmission in the neuropathic pain model, the increase of 5-HT$_{2C}$R would have to occur in the population of BLA cells that drive direct excitation of CeA neurons. The small and unchanged contribution of 5-HT$_{2C}$R to feedforward inhibition of CeA neurons under control conditions and in neuropathic pain would suggest the involvement of other mechanisms in the control of GABAergic interneurons, such as modulation by the medial prefrontal cortex (Cho et al., 2013). Our previous studies at the acute stage of the kaolin/carrageenan arthritis model showed decreased feedforward inhibition (Ren and Neugebauer, 2010; Ren et al., 2013). The contribution of 5-HT$_{2C}$R was not determined, but it is possible that differential effects of acute and chronic serotonin are involved (see the previous paragraph and Rainnie, 1999).

Amygdala 5-HT$_{2C}$R function beyond pain

The significance of this study extends beyond the field of pain research. 5-HT$_{2C}$R has emerged as a therapeutic target for neuropsychiatric disorders (Millan, 2005; Heisler et al., 2007; Christianson et al., 2010; Jensen et al., 2010), but also mediates anxiogenic side effects of acutely administered antidepressants such as SSRIs (Burghardt et al., 2007; Lee and Chen, 2010; Ravinder et al., 2011). Pointing to the amygdala as a site of action, a 5-HT$_{2C}$R antagonist (SB242084) in the BLA blocked the anxiogenic effects of systemic imipramine and fluoxetine (Vicente and Zangrossi, 2012). Evidence showing that anxiogenic effects of 5-HT$_{2C}$R agonists (MK-212 and CP-809101) in the BLA were decreased by chronic antidepressants (Vicente and Zangrossi, 2014) or by physical exercise (Greenwood et al., 2012) implicates decreased 5-HT$_{2C}$R function, possibly at the transcriptional level (reduced 5-HT$_{2C}$R mRNA), in antidepressant mechanisms.

The major source of 5-HT in the amygdala is the dorsal raphe nucleus and serotonergic fibers target primarily the lateral and basolateral nuclei, but not CeA or intercalated cells (Bombardi, 2014; Linley et al., 2017). There is evidence for increased 5-HT release in the BLA, but not CeA, in aversive states (Funada and Hara, 2001; Macedo et al., 2005; Christianson et al., 2010). Anxiogenic effects of 5-HT$_{2C}$R agonists in the BLA are well established. CP809101 in the BLA, but not CeA, increased anxiety-like behavior in the EPM (Pockros-Burgess et al., 2014). MK-212 in the BLA had anxiogenic effects in the elevated T-maze and in the light–dark transition test (Vicente and Zangrossi, 2014). RO 60–0175 induced an anxiogenic response in the open-field test (Moya et al., 2011). Likewise, increased expression of 5-HT$_{2C}$R in the amygdala with a viral vector strategy (5-HT$_{2C}$R promoter-controlled 5-HT$_{2C}$R sense sequence injected into the amygdala; Li et al., 2012) or using transgenic mice overexpressing 5-HT$_{2C}$R in the brain, including the amygdala, under the control of the CaMKIIa promoter (Kimura et al., 2009) produced anxiety-like behavior in the EPM. Conversely, a 5-HT$_{2C}$R antagonist (SB-242084) in the BLA had anxiolytic effects, impairing inhibitory avoidance in the elevated T-maze (Vicente and Zangrossi, 2012) and blocking poststress anxiety in a so-called juvenile social exploration test (Christianson et al., 2010). SB-242084 in the BLA also blocked the anxiogenic effect of systemic MK-212 in the EPM (de Mello Cruz et al., 2005).

Particularly relevant to our work is the observation that the anxiogenic effects of 5-HT$_{2C}$R are linked to the CRF system in the extended amygdala, including CeA. 5-HT$_{2C}$R knock-out mice showed an anxiolytic phenotype in the open-field and elevated zero maze tests and blunted activation (decreased c-Fos immunoreactivity) of corticotropin releasing factor (CRF)-containing neurons (Heisler et al., 2007). Importantly, the present study and our previous work focused on nonaccommodating regular spiking CeA neurons with parabrachial input (Neugebauer, 2015), which are characteristics of CRF-containing CeA neurons known to target brain/brainstem areas for behavioral modulation (McCall et al., 2015; Pomrenze et al., 2015). Direct excitatory CRF projections from CeA neurons to brainstem areas promote aversive and anxiety-like behaviors (Fendt et al., 1997; Reyes et al., 2011; Beckerman et al., 2013; McCall et al., 2015). Our results suggest that 5-HT$_{2C}$R in the BLA drives these CeA neurons to generate neuropathic-pain-related emotional-affective responses and anxiety- and depression-like behaviors. Amygdala-induced neuropathic pain behavior involves actions on regulatory centers in the brainstem such as the rostral ventromedial medulla directly or through the periaqueductal gray (Ansah et al., 2009) and locus ceruleus (Viisanen and Pertovaara, 2007), which are known direct targets of CRF-containing CeA neurons (Reyes et al., 2011; Penzo et al., 2014; McCall et al., 2015; Pomrenze et al., 2015).

Technical considerations

The viral vector that we used to knock down 5-HT$_{2C}$R has been validated in previous studies (Anastasio et al., 2014; Anastasio et al., 2015). Here, we show decreased 5-HT$_{2C}$R mRNA and immunoreactivity after focal injection of AAV-expressing 5-HT$_{2C}$R shRNA, but not control shRNA (Fig. 1). Control shRNA vector injected into BLA and offsite control injections of 5-HT$_{2C}$R shRNA vector into CeA had no behavioral and electrophysiological effects. Lack of effect of 5-HT$_{2C}$R knockdown in the BLA in

sham controls on behavior and on BLA-driven monosynaptic excitatory input to the CeA (Fig. 8*A*), the key outcome measure that changed in the pain model (Fig. 8*C*) and is known to account for amygdala-dependent pain behaviors (for review, see Neugebauer, 2015), argue against nonspecific cell damage, as does the lack of effect of offsite injections into the CeA. Lack of effects of CeA injections strongly support focal effects of BLA injections and point to the BLA as the site of action of 5-HT$_{2C}$R. The antibodies used to detect 5-HT$_{2C}$R are well established in the literature (Anastasio et al., 2014). It should also be noted that our systems and brain slice electrophysiology focused on a well defined subpopulation of amygdala/CeA neurons (see the previous paragraph) that are closely linked to pain modulation (Neugebauer, 2015), which may explain the quite consistent effect of 5-HT$_{2C}$R knockdown. Finally, confounding motoric activity changes need to be considered, but are unlikely to explain the behavioral effects of 5-HT$_{2C}$R knockdown in our study. Open- or closed-arm preference in the EPM would be equally affected by nonspecific or motoric changes and spinal reflexes and vocalizations increased in the pain model and decreased with 5-HT$_{2C}$R knockdown, whereas open-arm preference changed in the opposite direction.

Conclusions

The results of the present study suggest that increased 5-HT$_{2C}$R in the BLA contributes to neuropathic-pain-related behaviors by driving synaptic excitation of CeA neurons to increase amygdala output. We conclude that 5-HT$_{2C}$R knockdown in the BLA is an effective rescue strategy to inhibit amygdala activity and neuropathic-pain-related behaviors.

References

Adedoyin MO, Vicini S, Neale JH (2010) Endogenous N-acetylaspartylglutamate (NAAG) inhibits synaptic plasticity/transmission in the amygdala in a mouse inflammatory pain model. Mol Pain 6:60–77. CrossRef Medline

Anastasio NC, Stutz SJ, Fox RG, Sears RM, Emeson RB, DiLeone RJ, O'Neil RT, Fink LH, Li D, Green TA, Moeller FG, Cunningham KA (2014) Functional status of the serotonin 5-HT2C receptor (5-HT2CR) drives interlocked phenotypes that precipitate relapse-like behaviors in cocaine dependence. Neuropsychopharmacology 39:370–382. CrossRef Medline

Anastasio NC, Stutz SJ, Fink LH, Swinford-Jackson SE, Sears RM, DiLeone RJ, Rice KC, Moeller FG, Cunningham KA (2015) Serotonin (5-HT) 5-HT2A receptor (5-HT2AR):5-HT2CR imbalance in medial prefrontal cortex associates with motor impulsivity. ACS Chem Neurosci 6:1248–1258. CrossRef Medline

Ansah OB, Gonçalves L, Almeida A, Pertovaara A (2009) Enhanced pronociception by amygdaloid group I metabotropic glutamate receptors in nerve-injured animals. Exp Neurol 216:66–74. CrossRef Medline

Beckerman MA, Van Kempen TA, Justice NJ, Milner TA, Glass MJ (2013) Corticotropin-releasing factor in the mouse central nucleus of the amygdala: ultrastructural distribution in NMDA-NR1 receptor subunit expressing neurons as well as projection neurons to the bed nucleus of the stria terminalis. Exp Neurol 239:120–132. CrossRef Medline

Bennett GJ, Chung JM, Honore M, Seltzer Z (2003) Models of neuropathic pain in the rat. Curr Protoc Neurosci Chapter 9:Unit 9.14.1. CrossRef Medline

Bird GC, Lash LL, Han JS, Zou X, Willis WD, Neugebauer V (2005) Protein kinase A-dependent enhanced NMDA receptor function in pain-related synaptic plasticity in rat amygdala neurones. J Physiol 564:907–921. CrossRef Medline

Bocchio M, McHugh SB, Bannerman DM, Sharp T, Capogna M (2016) Serotonin, amygdala and fear: assembling the puzzle. Front Neural Circuits 10:24. CrossRef Medline

Bockaert J, Claeysen S, Bécamel C, Dumuis A, Marin P (2006) Neuronal 5-HT metabotropic receptors: fine-tuning of their structure, signaling, and roles in synaptic modulation. Cell Tissue Res 326:553–572. CrossRef Medline

Bombardi C (2014) Neuronal localization of the 5-HT2 receptor family in the amygdaloid complex. Front Pharmacol 5:68. Medline

Brasch-Andersen C, Møller MU, Christiansen L, Thinggaard M, Otto M, Brøsen K, Sindrup SH (2011) A candidate gene study of serotonergic pathway genes and pain relief during treatment with escitalopram in patients with neuropathic pain shows significant association to serotonin receptor2C (HTR2C). Eur J Clin Pharmacol 67:1131–1137. CrossRef Medline

Bubar MJ, Stutz SJ, Cunningham KA (2011) 5-HT(2C) receptors localize to dopamine and GABA neurons in the rat mesoaccumbens pathway. PLoS One 6:e20508. CrossRef Medline

Burghardt NS, Bush DE, McEwen BS, LeDoux JE (2007) Acute selective serotonin reuptake inhibitors increase conditioned fear expression: blockade with a 5-HT(2C) receptor antagonist. Biol Psychiatry 62:1111–1118. CrossRef Medline

Campbell BM, Merchant KM (2003) Serotonin 2C receptors within the basolateral amygdala induce acute fear-like responses in an open-field environment. Brain Res 993:1–9. CrossRef Medline

Carr DB, Cooper DC, Ulrich SL, Spruston N, Surmeier DJ (2002) Serotonin receptor activation inhibits sodium current and dendritic excitability in prefrontal cortex via a protein kinase C-dependent mechanism. J Neurosci 22:6846–6855. Medline

Carrasquillo Y, Gereau RW 4th (2007) Activation of the extracellular signal-regulated kinase in the amygdala modulates pain perception. J Neurosci 27:1543–1551. CrossRef Medline

Carrasquillo Y, Gereau RW 4th (2008) Hemispheric lateralization of a molecular signal for pain modulation in the amygdala. Mol Pain 4:24. CrossRef Medline

Chaplan SR, Bach FW, Pogrel JW, Chung JM, Yaksh TL (1994) Quantitative assessment of tactile allodynia in the rat paw. J Neurosci Methods 53:55–63. CrossRef Medline

Chen A, Hough CJ, Li H (2003) Serotonin type II receptor activation facilitates synaptic plasticity via N-methyl-D-aspartate-mediated mechanism in the rat basolateral amygdala. Neuroscience 119:53–63. CrossRef Medline

Cheng SJ, Chen CC, Yang HW, Chang YT, Bai SW, Chen CC, Yen CT, Min MY (2011) Role of extracellular signal-regulated kinase in synaptic transmission and plasticity of a nociceptive input on capsular central amygdaloid neurons in normal and acid-induced muscle pain mice. J Neurosci 31:2258–2270. CrossRef Medline

Cho JH, Deisseroth K, Bolshakov VY (2013) Synaptic encoding of fear extinction in mPFC-amygdala circuits. Neuron 80:1491–1507. CrossRef Medline

Christianson JP, Ragole T, Amat J, Greenwood BN, Strong PV, Paul ED, Fleshner M, Watkins LR, Maier SF (2010) 5-hydroxytryptamine 2C receptors in the basolateral amygdala are involved in the expression of anxiety after uncontrollable traumatic stress. Biol Psychiatry 67:339–345. CrossRef Medline

Clemett DA, Punhani T, Duxon MS, Blackburn TP, Fone KC (2000) Immunohistochemical localisation of the 5-HT2C receptor protein in the rat CNS. Neuropharmacology 39:123–132. CrossRef Medline

de Mello Cruz AP, Pinheiro G, Alves SH, Ferreira G, Mendes M, Faria L, Macedo CE, Motta V, Landeira-Fernandez J (2005) Behavioral effects of systemically administered MK-212 are prevented by ritanserin microinfusion into the basolateral amygdala of rats exposed to the elevated plus-maze. Psychopharmacology (Berl) 182:345–354. CrossRef Medline

Dixon WJ (1980) Efficient analysis of experimental observations. Annu Rev Pharmacol Toxicol 20:441–462. CrossRef Medline

Duvarci S, Pare D (2014) Amygdala microcircuits controlling learned fear. Neuron 82:966–980. CrossRef Medline

Dworkin RH et al (2010) Recommendations for the pharmacological management of neuropathic pain: an overview and literature update. Mayo Clin Proc 85:S3–14. CrossRef Medline

Fendt M, Koch M, Schnitzler HU (1997) Corticotropin-releasing factor in the caudal pontine reticular nucleus mediates the expression of fear-potentiated startle in the rat. Eur J Neurosci 9:299–305. CrossRef Medline

Fernandez SP, Cauli B, Cabezas C, Muzerelle A, Poncer JC, Gaspar P (2016) Multiscale single-cell analysis reveals unique phenotypes of raphe 5-HT neurons projecting to the forebrain. Brain Struct Funct 221:4007–4025. Medline

Fernando AB, Robbins TW (2011) Animal models of neuropsychiatric disorders. Annu Rev Clin Psychol 7:39–61. CrossRef Medline

Finnerup NB, Attal N, Haroutounian S, McNicol E, Baron R, Dworkin RH, Gilron I, Haanpää M, Hansson P, Jensen TS, Kamerman PR, Lund K, Moore A, Raja SN,

Rice AS, Rowbotham M, Sena E, Siddall P, Smith BH, Wallace M (2015) Pharmacotherapy for neuropathic pain in adults: a systematic review and meta-analysis. Lancet Neurol 14:162–173. CrossRef Medline

Fu Y, Neugebauer V (2008) Differential mechanisms of CRF1 and CRF2 receptor functions in the amygdala in pain-related synaptic facilitation and behavior. J Neurosci 28:3861–3876. CrossRef Medline

Funada M, Hara C (2001) Differential effects of psychological stress on activation of the 5-hydroxytryptamine- and dopamine-containing neurons in the brain of freely moving rats. Brain Res 901:247–251. CrossRef Medline

Godlewska BR, Norbury R, Selvaraj S, Cowen PJ, Harmer CJ (2012) Short-term SSRI treatment normalises amygdala hyperactivity in depressed patients. Psychol Med 42:2609–2617. CrossRef Medline

Gonçalves L, Dickenson AH (2012) Asymmetric time-dependent activation of right central amygdala neurones in rats with peripheral neuropathy and pregabalin modulation. Eur J Neurosci 36:3204–3213. CrossRef Medline

Gonçalves L, Silva R, Pinto-Ribeiro F, Pêgo JM, Bessa JM, Pertovaara A, Sousa N, Almeida A (2008) Neuropathic pain is associated with depressive behaviour and induces neuroplasticity in the amygdala of the rat. Exp Neurol 213:48–56. CrossRef Medline

Greenwood BN, Strong PV, Loughridge AB, Day HE, Clark PJ, Mika A, Hellwinkel JE, Spence KG, Fleshner M (2012) 5-HT2C receptors in the basolateral amygdala and dorsal striatum are a novel target for the anxiolytic and antidepressant effects of exercise. PLoS One 7:e46118. CrossRef Medline

Grégoire S, Neugebauer V (2013) 5-HT2CR blockade in the amygdala conveys analgesic efficacy to SSRIs in a rat model of arthritis pain. Mol Pain 9:41. CrossRef Medline

Han JS, Neugebauer V (2004) Synaptic plasticity in the amygdala in a visceral pain model in rats. Neurosci Lett 361:254–257. CrossRef Medline

Han JS, Bird GC, Li W, Jones J, Neugebauer V (2005a) Computerized analysis of audible and ultrasonic vocalizations of rats as a standardized measure of pain-related behavior. J Neurosci Methods 141:261–269. CrossRef Medline

Han JS, Li W, Neugebauer V (2005b) Critical role of calcitonin gene-related peptide 1 receptors in the amygdala in synaptic plasticity and pain behavior. J Neurosci 25:10717–10728. CrossRef Medline

Hannon J, Hoyer D (2008) Molecular biology of 5-HT receptors. Behav Brain Res 195:198–213. CrossRef Medline

Heinricher MM, Tavares I, Leith JL, Lumb BM (2009) Descending control of nociception: Specificity, recruitment and plasticity. Brain Res Rev 60:214–225. CrossRef Medline

Heisler LK, Zhou L, Bajwa P, Hsu J, Tecott LH (2007) Serotonin 5-HT(2C) receptors regulate anxiety-like behavior. Genes Brain Behav 6:491–496. CrossRef Medline

Holt GR, Softky WR, Koch C, Douglas RJ (1996) Comparison of discharge variability in vitro and in vivo in cat visual cortex neurons. J Neurophysiol 75:1806–1814. Medline

Ikeda R, Takahashi Y, Inoue K, Kato F (2007) NMDA receptor-independent synaptic plasticity in the central amygdala in the rat model of neuropathic pain. Pain 127:161–172. CrossRef Medline

Janak PH, Tye KM (2015) From circuits to behaviour in the amygdala. Nature 517:284–292. CrossRef Medline

Jensen NH, Cremers TI, Sotty F (2010) Therapeutic potential of 5-HT2C receptor ligands. ScientificWorldJournal 10:1870–1885. CrossRef Medline

Ji G, Neugebauer V (2009) Hemispheric lateralization of pain processing by amygdala neurons. J Neurophysiol 1102:2253–2264. CrossRef Medline

Ji G, Fu Y, Ruppert KA, Neugebauer V (2007) Pain-related anxiety-like behavior requires CRF1 receptors in the amygdala. Mol Pain 3:13–17. CrossRef Medline

Ji G, Sun H, Fu Y, Li Z, Pais-Vieira M, Galhardo V, Neugebauer V (2010) Cognitive impairment in pain through amygdala-driven prefrontal cortical deactivation. J Neurosci 30:5451–5464. CrossRef Medline

Ji G, Fu Y, Adwanikar H, Neugebauer V (2013) Non-pain-related CRF1 activation in the amygdala facilitates synaptic transmission and pain responses. Mol Pain 9:2. CrossRef Medline

Ji G, Li Z, Neugebauer V (2015) Reactive oxygen species mediate visceral pain-related amygdala plasticity and behaviors. Pain 156:825–836. CrossRef Medline

Kimura A, Stevenson PL, Carter RN, Maccoll G, French KL, Simons JP, Al-Shawi R, Kelly V, Chapman KE, Holmes MC (2009) Overexpression of 5-HT2C receptors in forebrain leads to elevated anxiety and hypoactivity. Eur J Neurosci 30:299–306. CrossRef Medline

Lee YC, Chen PP (2010) A review of SSRIs and SNRIs in neuropathic pain. Expert Opin Pharmacother 11:2813–2825. CrossRef Medline

Li Q, Luo T, Jiang X, Wang J (2012) Anxiolytic effects of 5-HT(1)A receptors and anxiogenic effects of 5-HT(2)C receptors in the amygdala of mice. Neuropharmacology 62:474–484. CrossRef Medline

Linley SB, Olucha-Bordonau F, Vertes RP (2017) Pattern of distribution of serotonergic fibers to the amygdala and extended amygdala in the rat. J Comp Neurol 525:116–139. CrossRef Medline

Liu S, Bubar MJ, Lanfranco MF, Hillman GR, Cunningham KA (2007) Serotonin(2C) receptor localization in GABA neurons of the rat medial prefrontal cortex: Implications for understanding the neurobiology of addiction. Neuroscience 146:1677–1688. CrossRef Medline

Lowry CA (2002) Functional subsets of serotonergic neurones: implications for control of the hypothalamic-pituitary-adrenal axis. J Neuroendocrinol 14:911–923. CrossRef Medline

Ma QP, Yin GF, Ai MK, Han JS (1991) Serotonergic projections from the nucleus raphe dorsalis to the amygdala in the rat. Neurosci Lett 134:21–24. CrossRef Medline

Macedo CE, Martinez RC, de Souza Silva MA, Brandão ML (2005) Increases in extracellular levels of 5-HT and dopamine in the basolateral, but not in the central, nucleus of amygdala induced by aversive stimulation of the inferior colliculus. Eur J Neurosci 21:1131–1138. CrossRef Medline

McCall JG, Al-Hasani R, Siuda ER, Hong DY, Norris AJ, Ford CP, Bruchas MR (2015) CRH engagement of the locus coeruleus noradrenergic system mediates stress-induced anxiety. Neuron 87:605–620. CrossRef Medline

McDonald AJ (1998) Cortical pathways to the mammalian amygdala. Prog Neurobiol 55:257–332. CrossRef Medline

Millan MJ (2005) Serotonin 5-HT2C receptors as a target for the treatment of depressive and anxious states: focus on novel therapeutic strategies. Therapie 60:441–460. CrossRef Medline

Millan MJ, Marin P, Bockaert J, Mannoury la Cour C (2008) Signaling at G-protein-coupled serotonin receptors: recent advances and future research directions. Trends Pharmacol Sci 29:454–464. CrossRef Medline

Moya PR, Fox MA, Jensen CL, Laporte JL, French HT, Wendland JR, Murphy DL (2011) Altered 5-HT2C receptor agonist-induced responses and 5-HT2C receptor RNA editing in the amygdala of serotonin transporter knockout mice. BMC Pharmacol 11:3. CrossRef Medline

Muller JF, Mascagni F, McDonald AJ (2007) Serotonin-immunoreactive axon terminals innervate pyramidal cells and interneurons in the rat basolateral amygdala. J Comp Neurol 505:314–335. CrossRef Medline

Nakao A, Takahashi Y, Nagase M, Ikeda R, Kato F (2012) Role of capsaicin-sensitive C-fiber afferents in neuropathic pain-induced synaptic potentiation in the nociceptive amygdala. Mol Pain 8:51. CrossRef Medline

Neugebauer V (2015) Amygdala pain mechanisms. Handb Exp Pharmacol 227:261–284. CrossRef Medline

Neugebauer V, Li W, Bird GC, Bhave G, Gereau RW 4th (2003) Synaptic plasticity in the amygdala in a model of arthritic pain: differential roles of metabotropic glutamate receptors 1 and 5. J Neurosci 23:52–63. Medline

Neugebauer V, Li W, Bird GC, Han JS (2004) The amygdala and persistent pain. Neuroscientist 10:221–234. CrossRef Medline

Neugebauer V, Han JS, Adwanikar H, Fu Y, Ji G (2007) Techniques for assessing knee joint pain in arthritis. Mol Pain 3:8–20. CrossRef Medline

Nusser Z, Naylor D, Mody I (2001) Synapse-specific contribution of the variation of transmitter concentration to the decay of inhibitory postsynaptic currents. Biophys J 80:1251–1261. CrossRef Medline

Ossipov MH, Dussor GO, Porreca F (2010) Central modulation of pain. J Clin Invest 120:3779–3787. CrossRef Medline

Parent A, Descarries L, Beaudet A (1981) Organization of ascending serotonin systems in the adult rat brain. A radioautographic study after intraventricular administration of [3H]5-hydroxytryptamine Neuroscience 6:115–138. Medline

Penzo MA, Robert V, Li B (2014) Fear conditioning potentiates synaptic transmission onto long-range projection neurons in the lateral subdivision of central amygdala. J Neurosci 34:2432–2437. CrossRef Medline

Phelps EA, LeDoux JE (2005) Contributions of the amygdala to emotion processing: from animal models to human behavior. Neuron 48:175–187. CrossRef Medline

Pockros-Burgess LA, Pentkowski NS, Der-Ghazarian T, Neisewander JL (2014) Effects of the 5-HT2C receptor agonist CP809101 in the amygdala on reinstatement of cocaine-seeking behavior and anxiety-like behavior. Int J Neuropsychopharmacol 17:1751–1762. CrossRef Medline

Pompeiano M, Palacios JM, Mengod G (1994) Distribution of the serotonin 5-HT$_2$ receptor family mRNAs: comparison between 5-HT$_{2A}$ and 5-HT$_{2C}$ receptors. Mol Brain Res 23:163–178. CrossRef Medline

Pomrenze MB, Millan EZ, Hopf FW, Keiflin R, Maiya R, Blasio A, Dadgar J, Kharazia V, De Guglielmo G, Crawford E, Janak PH, George O, Rice KC, Messing RO (2015) A transgenic rat for investigating the anatomy and function of corticotrophin releasing factor circuits. Front Neurosci 9:487. Medline

Rainnie DG (1999) Serotonergic modulation of neurotransmission in the rat basolateral amygdala. J Neurophysiol 82:69–85. Medline

Ravinder S, Pillai AG, Chattarji S (2011) Cellular correlates of enhanced anxiety caused by acute treatment with the selective serotonin reuptake inhibitor fluoxetine in rats. Front Behav Neurosci 5:88. CrossRef Medline

Ren W, Neugebauer V (2010) Pain-related increase of excitatory transmission and decrease of inhibitory transmission in the central nucleus of the amygdala are mediated by mGluR1. Mol Pain 6:93–106. CrossRef Medline

Ren W, Kiritoshi T, Grégoire S, Ji G, Guerrini R, Calo G, Neugebauer V (2013) Neuropeptide S: a novel regulator of pain-related amygdala plasticity and behaviors. J Neurophysiol 110:1765–1781. CrossRef Medline

Reyes BA, Carvalho AF, Vakharia K, Van Bockstaele EJ (2011) Amygdalar peptidergic circuits regulating noradrenergic locus coeruleus neurons: linking limbic and arousal centers. Exp Neurol 230:96–105. CrossRef Medline

Ryan SJ, Ehrlich DE, Jasnow AM, Daftary S, Madsen TE, Rainnie DG (2012) Spike-timing precision and neuronal synchrony are enhanced by an interaction between synaptic inhibition and membrane oscillations in the amygdala. PLoS One 7:e35320. CrossRef Medline

Sah P, Faber ES, Lopez De Armentia M, Power J (2003) The amygdaloid complex: anatomy and physiology. Physiol Rev 83:803–834. CrossRef Medline

Vicente MA, Zangrossi H (2012) Serotonin-2C receptors in the basolateral nucleus of the amygdala mediate the anxiogenic effect of acute imipramine and fluoxetine administration. Int J Neuropsychopharmacol 15:389–400. CrossRef Medline

Vicente MA, Zangrossi H Jr (2014) Involvement of 5-HT2C and 5-HT1A receptors of the basolateral nucleus of the amygdala in the anxiolytic effect of chronic antidepressant treatment. Neuropharmacology 79:127–135. CrossRef Medline

Viisanen H, Pertovaara A (2007) Influence of peripheral nerve injury on response properties of locus coeruleus neurons and coeruleospinal antinociception in the rat. Neuroscience 146:1785–1794. CrossRef Medline

Walf AA, Frye CA (2007) The use of the elevated plus maze as an assay of anxiety-related behavior in rodents. Nat Protoc 2:322–328. CrossRef Medline

Wang W, Jones HE, Andolina IM, Salt TE, Sillito AM (2006) Functional alignment of feedback effects from visual cortex to thalamus. Nat Neurosci 9:1330–1336. CrossRef Medline

Weyand TG, Boudreaux M, Guido W (2001) Burst and tonic response modes in thalamic neurons during sleep and wakefulness. J Neurophysiol 85:1107–1118. Medline

Zhang Y, Crofton EJ, Li D, Lobo MK, Fan X, Nestler EJ, Green TA (2014) Overexpression of DeltaFosB in nucleus accumbens mimics the protective addiction phenotype, but not the protective depression phenotype of environmental enrichment. Front Behav Neurosci 8:297. CrossRef Medline